WYLE LABORATORIES - RESEARCH STAFF
Report WR 66-17

Errata

RESPONSE OF PANELS TO OSCILLATING
SHOCK WAVES

by
M. J. Crocker

1.   Replace Figure 1, page 47, with new page attached.

2.   In Figure 5, page 51, alter caption of the ordinate from "Dynamic Magnification
Factor for First Mode" to "First Mode Dynamic Displacement/Displacement Due to
Same Uniformly Distributed Static Load".

WYLE LABORATORIES - RESEARCH STAFF
Report WR 66-17

RESPONSE OF PANELS TO OSCILLATING SHOCK WAVES

By
M. J. Crocker

March, 1966

COPY NO._____

WYLE LABORATORIES - RESEARCH STAFF
Report WR 66-17

RESPONSE OF PANELS TO OSCILLATING
SHOCK WAVES

By
M. J. Crocker

Submitted under
Brown Engineering Co. Work Order No. 933-50-19-9132
Technical Directive W-25
NASA Contract No. NAS3-20073-1

Prepared by _M. J. Crocker_
M. J. Crocker

Approved by _L. C. Sutherland_
L. C. Sutherland

Approved by _K. McK. Eldred_
K. McK. Eldred
Director of Research

Date   March, 1966

SUMMARY

Experimental data of oscillating shock waves experienced by space vehicles are examined to determine whether shocks oscillate in a random or discrete manner. Since there is evidence to suggest that shocks can oscillate at discrete frequencies, this was chosen as the principal theoretical model. Theory is formulated for the response of a simply-supported panel to sinusoidally oscillating shocks and to shocks moving at constant speed. Some analysis of the theory is made and it is found that first mode dynamic amplification factors as high as fifty could be experienced by a panel for a shock oscillating about the panel center, over the full span and at the panel resonant frequency, for typical panel damping.

TABLE OF CONTENTS

LIST OF FIGURES

LIST OF TABLES

LIST OF SYMBOLS

a	panel length in x - direction
A	modal constant
A	panel surface area
A	dynamic amplification factor
b	panel width in y - direction
B	modal constant
C	modal constant
C	generalized damping coefficient
D	modal constant
D	mean position of oscillating shock front
$\bar{D}$	D/a, non-dimensionalized mean position of oscillating shock front
e	2.718, base of natural numbers
e	strain
E	Young's Modulus
f_r	normalized r^{th} mode shape of panel
G	total displacement of any point on panel
h	panel thickness
H	amplitude of shock oscillation
$\bar{H}$	H/a, non-dimensionalized amplitude of shock oscillation
J_0	Bessel function of the first kind, zero order
J_{2k}	Bessel function of the first kind, $2k^{th}$ order
J_{2k+1}	Bessel function of the first kind, $(2k+1)^{th}$ order
K	generalized stiffness
ℓ	position of shock front
L	generalized force
m	mode number in x - direction
M	generalized mass
M	Mach number

LIST OF SYMBOLS (CONTINUED)

n	mode number in y – direction
p	pressure
p_0	peak pressure
q	dynamic pressure
t	time
u	particle velocity
v	velocity of shock front
x	panel length in x – direction
X	modal function of x or y
|X|	maximum value of X
y	panel length in y – direction
z	$\sigma \sigma$

Greek Alphabet

α	frequency parameter
α	angular frequency of shock wave oscillations
β	α/ω , ratio of shock wave frequency to natural frequency of panel
γ	ratio of specific heats for air
δ	critical damping ratio
μ	$m\pi H/a$
ν	Poisson's ratio
ξ	generalized modal displacement coordinate
ρ	density of material
σ	tensile stress
σ	"dummy" time variable
$\bar{\sigma}$	at , non-dimensionalized "dummy" time
τ	duration of impulsive force
ψ	resonant frequency parameter
ω	angular resonant frequency of panel

LIST OF SYMBOLS (CONTINUED)

Subscripts

0	refers to natural undamped resonant frequency
A	refers to time regime A
B	refers to time regime B
d	refers to damped natural resonant frequency
m	refers to m^{th} mode
n	refers to n^{th} mode
osc	refers to oscillating shock
static	refers to suddenly applied uniform load
r	refers to r^{th} mode
x	refers to x – direction
y	refers to y – direction

1.0 INTRODUCTION

As a typical space vehicle accelerates through the atmosphere it is subjected to fluctuating pressure loads on the vehicle skin due to a variety of aerodynamic mechanisms. These pressure loadings can be so severe that they have caused the loss of some vehicles (Reference 1). Thus, it is imperative that the loading which a prototype vehicle will experience and the effects upon the structure must be estimated before its first flight. Figure 1 (extracted from Reference 2) shows the relative importance of the fluctuating pressure loadings experienced by a typical launch vehicle. It is seen that, except during the initial 10 or 20 seconds of flight when structural loading caused by the noise from the rocket exhaust mixing with the atmosphere predominates, the dominant loading is caused by pressure fluctuations due to the turbulent boundary layer and separated and wake flows which are often coupled with oscillating shock waves.

Although these latter aerodynamic phenomena are coupled together, calculating the response of the missile structure to such a combined loading would be very difficult. The normal procedure is to assume that each loading is uncoupled. The structural response to each source of excitation is then calculated and the total response found by a summation of responses. This affords a considerable simplification in the mathematics. In this report, only the response of structure to traveling shocks is considered.

Experimental evidence shows that during supersonic flight of a missile, separated flow and shock waves occur at the interstage farings where the stream lines encounter local compression. During the subsonic flight regime the separated flow and shock waves form at the shoulders of the vehicle where local compression is encountered by the flow. As the vehicle accelerates, these shock waves tend to oscillate and simultaneously run down the vehicle from one flare or shoulder to the next. Thus, the response of vehicle structure, to both running and oscillating shock waves, is of interest.

In Section 2 of this report, available experimental evidence is examined to decide the manner in which shock waves oscillate. In Section 3.1, theory for the response of a panel to a time varying force is formulated. Section 3.2 deals with panel response to grazing incidence moving shocks and in Section 3.3, theory is formulated for panel response to a grazing incidence shock moving with constant velocity. In Section 3.4, the theory is extended to cover the case of panel response to grazing incidence sinusoidally oscillating shocks, where the amplitude of shock oscillation is restricted. Section 4.0 of this report deals with computations made of the analysis of Section 3.4

Equation (1) below gives the ratio of static pressures across a shock front in terms of the Mach number of the approaching flow, M_1 .

$$\frac{P_2}{P_1} = \frac{\left[2\gamma M_1^2 - (\gamma - 1)\right]}{\gamma + 1} \tag{1}$$

1

where γ is the ratio of specific heats of air.

The notation used is shown in the sketch below, which shows an idealized normal attached shock wave.
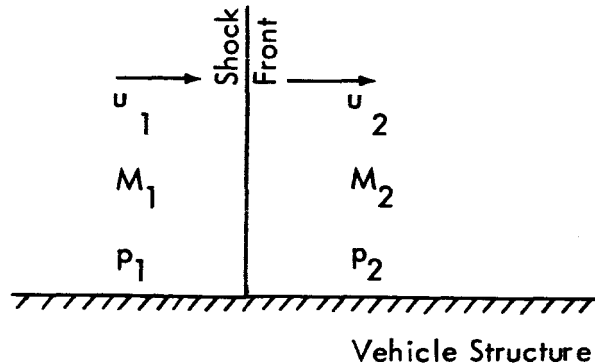
Vehicle Structure

If the shock wave oscillates relative to the vehicle structure, the pressure p_2 does not remain constant, but increases as the shock front moves upstream and decreases as it moves downstream. The static pressure p_2 can only be assumed to remain constant provided the shock front velocity remains small compared with the velocity u_1 of the approaching flow.

In Appendix A, a method which can be used to allow for this change in pressure and velocity, if necessary, is formulated. It is not necessary, in this case, to introduce the approximations made in Section 3.4 and thus, there is no restriction on the amplitude of oscillation. The theory formulated allows both sinusoidally oscillating shocks and shocks oscillating at constant speed to be considered.

Appendix B shows how the theory developed in Section 3.4 can be formulated without the restriction on amplitude of the oscillating shock. Appendix C shows how the analyses, which have hitherto been restricted to simply-supported panels throughout the report, can be developed for the case of clamped-clamped panels. Appendix D gives the logic for the computer program used for computation of the analysis of Section 3.4.

2.0   DISCUSSION ON BEHAVIOR OF OSCILLATING SHOCKS

2.1   Examination of Experimental Data on Shock Oscillation

It is a well known fact that the shock waves which form around aircraft and space vehicles during transonic and supersonic flight in the atmosphere are not stationary but oscillatory in nature. As a flight vehicle accelerates through the transonic regime of its flight, the shocks run backwards down the vehicle skin and oscillate simultaneously in some manner. With high speed aircraft the annoying phenomenon known as "aileron buzz" has been experienced for many years; in the case of space vehicles, the unsteady loading caused by the running and oscillating shocks is more serious.

The shocks which occur on a typical space vehicle form about the shoulders and flares of the vehicle. These shocks are aerodynamically coupled with the turbulent boundary layer and separated flows at these points. Calculating the vehicle skin response to such a coupled unsteady pressure field would be a very complicated task. However, if it is assumed that the pressure field due to these coupled phenomena can be separated, then the vehicle skin response can be determined for each forcing function, and the actual skin response found by summing the responses. This approach affords a great simplification in the mathematics and is adopted in this report.

Although it is well known that the shocks are oscillating in nature, evidence as to the nature and type of oscillations is sparse and the measurements that have been taken, often suggest conflicting physical models. This is probably due to the complex coupled nature of the flows and the probability that different data have been gathered from entirely different flow regimes.

In Reference 3, an attempt was made to set up an oscillating shock in a wind tunnel (at $M \simeq 2$) with the use of an oscillating aerofoil. The acoustic measurements indicated that the turbulent boundary layer pressure frequency spectrum was increased over a broad band with no evidence of discrete frequencies present; however, these could have been masked since there was much tunnel noise present. In Reference 2, Krause indicated that oscillating shocks may have been responsible for discrete frequencies found at about 200 and 220 cps during the Saturn SA-4 flight. In Reference 4, experimental work by Kistler revealed the existence of discrete frequency oscillations of a shock wave associated with a separated flow region at supersonic Mach numbers. However, repetition of this same work by Coe, at Ames A.F.B., did not reveal the same discrete frequencies but suggested that the shock wave simply magnified the pressure fluctuations of the turbulent boundary layer. In Reference 5, during recent sled tests at Holloman A.F.B., the existence of discrete frequencies of about 215 and 430 cps has been observed on a flat plate at transonic Mach numbers ($M \simeq 0.84$).

In References 6 and 7, Lowson suggests that the shock wave is very quick to couple with any forcing frequency present in the local environment. Such a forcing function could result from resonances of the panel or from discrete frequencies present in the turbulent boundary layer pressure frequency spectrum. Lowson also makes the interesting suggestion

(which has also been made previously by other authors) that the peak pressure fluctuations beneath the shock are due to shock-turbulence interactions.

As there is much evidence that a shock can oscillate at a discrete frequency, this case will be considered in the following sections of the report, particularly since the structural response problem is probably more easily analyzed and set up for digital computation than for the randomly oscillating shock case.

2.2   Definition of a Theoretical Model for Shock Oscillation
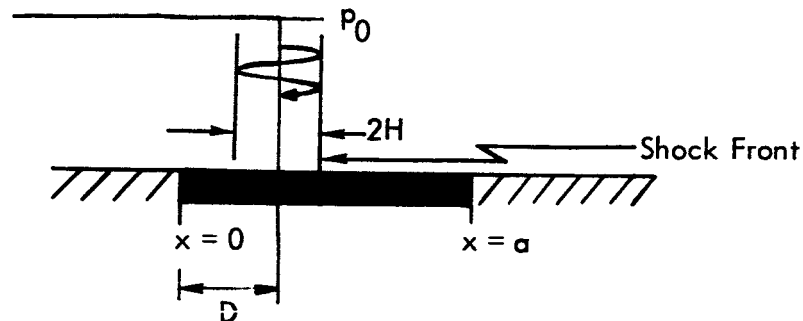
The oscillating shocks which are .examined later in this report, can be considered to oscillate about a mean position x = D on the panel, in a direction parallel to two sides of the panel. If the amplitude of vibration is H, then the position of the shock front at any time t may be given by:

$$X = D + H \sin \alpha \, t \tag{2}$$

if α is the angular frequency of vibration.

3.0 PANEL RESPONSE TO OSCILLATING SHOCKS

3.1 Panel Response to a Time Dependent Force

If the case of small viscous damping for a panel is assumed, cross coupling of the modes due to damping may be ignored and the well known Lagrange equation of motion (Equation 3) may be written:

$$M_r \ddot{\xi}_r(t) + C_r \dot{\xi}_r(t) + K_r \xi_r(t) = L_r(t) \tag{3}$$

where: $\xi_r(t)$ is the generalized displacement coordinate at time t

M_r is the generalized mass $= \rho h \iint\limits_{x\,y} f_r(x,y)\, dx\, dy$

C_r is the generalized damping coefficient $= 2 M_r \omega_r \delta_r$

K_r is the generalized stiffness $= M_r \omega_r^2$

$L_r(t)$ is the generalized force at time $t = \iint\limits_{x\,y} p(x,y,t) f_r(x,y)\, dx\, dy$

$f_r(x,y)$ is the mode shape

h is the panel thickness

$p(x,y,t)$ is the spatial pressure time history

δ_r is the critical damping ratio

ρ is the density of the panel material

ω_r is the angular resonant undamped frequency

Subscript r refers to the rth mode

Equations (3) describe the effective motion of a set of independent single degree of freedom systems.

The total displacement at any point (x,y) on the panel and at any time t is given by:

$$G(x,y,t) = \sum_{r=1}^{\infty} \left[\xi_r(t) f_r(x,y) \right] \tag{4}$$

5

The displacement $G(x,y,t)$ is the sum of the products of the generalized displacement co-ordinate and the mode shape of each mode. Normally it is found that only the first few modes provide significant contributions to the panel displacement and that the contributions of the higher modes are negligible.

The strains in the x- and y- directions, $e_x(x,y,t)$ and $e_y(x,y,t)$, respectively, are given by equations (5) and (6), by considering simple bending theory (Reference 8):

$$e_x(x,y,t) = -\frac{h}{2} \cdot \frac{\partial^2}{\partial x^2} \left[G(x,y,t) \right] \tag{5}$$

$$e_y(x,y,t) = -\frac{h}{2} \cdot \frac{\partial^2}{\partial y^2} \left[G(x,y,t) \right] \tag{6}$$

It is found that more modes must be considered in the case of the strain time history, than in the case of the displacement time history in order to obtain the same accuracy in the response time history.

The stresses $\sigma_x(x,y,t)$ and $\sigma_y(x,y,t)$ in the x- and y- directions, respectively, for a point x,y on the panel at time t are given by:

$$\sigma_x(x,y,t) = \frac{E}{(1-\nu^2)} \left[e_x(x,y,t) + \nu\, e_y(x,y,t) \right] \tag{7}$$

$$\sigma_y(x,y,t) = \frac{E}{(1-\nu^2)} \left[e_y(x,y,t) + \nu\, e_x(x,y,t) \right] \tag{8}$$

where E is Young's Modulus of Elasticity
ν is Poisson's Ratio

If $L_r(t) = 0$ in Equation (3), the solution is given (see Reference 9) by:

$$\xi_r(t) = e^{-\frac{C_r t}{2M_r}} \left[\xi_{0_r} \cos\omega_{d_r} t + \left(\dot{\xi}_{0_r} + \frac{C}{2M} \xi_{0_r} \right) \frac{\sin\omega_{d_r} t}{\omega_{d_r}} \right] \tag{9}$$

provided the damping is subcritical $(K_r > C_r^2 / 4M_r)$.

where ξ_{0_r} is the initial displacement in the rth mode

and $\dot{\xi}_{0_r}$ is the initial velocity in the rth mode

6
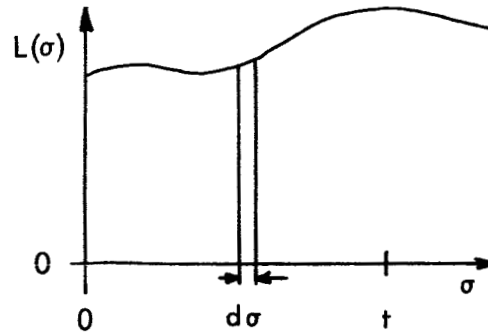
If the panel is subjected to an elemental impulse at time σ of $L(\sigma)\, d\sigma$, as shown in the above figure, then the generalized displacement in the rth mode, due to the generalized r^{th} modal impulse $L_r(\sigma)\, d\sigma$ is:

$$d\xi_r(t) = e^{-\dfrac{C_r(t-\sigma)}{2M_r}} \left[\dfrac{L_r(\sigma)\sin\omega_{d_r}(t-\sigma)}{M_r \omega_{d_r}} \right] d\sigma \tag{10}$$

This equation was obtained by substituting the incremental velocity $d\dot{\xi}_{0_r} = \dfrac{L_r(\sigma)\, d\sigma}{M_r}$

into Equation (9) and putting $\xi_{0_r} = 0$. Thus the generalized coordinate at time t due to the continuous application of the force $L(\sigma)$ is

$$\xi_r(t) = \dfrac{1}{M_r \omega_{d_r}} \int_0^t L_r(\sigma)\, e^{-\dfrac{C_r}{2M_r}(t-\sigma)} \sin\omega_{d_r}(t-\sigma)\, d\sigma \tag{11}$$

Equation (11) is often termed the Duhamel or convolution integral.

In order to determine the complete solution of Equation (3), it is necessary to add Equations (9) and (11) together. Thus the generalized displacement coordinate:

$$\xi_r(t) = e^{-\dfrac{C_r t}{2M}} \left[\xi_{0_r} \cos\omega_{d_r} t + \left(\dot{\xi}_{0_r} + \dfrac{C_r}{2M} \xi_{0_r} \right) \dfrac{\sin\omega_{d_r} t}{\omega_{d_r}} \right] +$$

$$+ \dfrac{1}{M_r \omega_{d_r}} \int_0^t L_r(\sigma)\, e^{-\dfrac{C_r}{2M_r}(t-\sigma)} \sin\omega_{d_r}(t-\sigma)\, d\sigma \tag{12}$$

7

The first term in this equation represents the effect of initial displacement and velocity, while the last term represents the effect of the disturbing force.

If the initial displacement and velocity are assumed zero, then Equation (12) may be rewritten:

$$\xi_r(t) = \frac{1}{M_r \omega_{d_r}} \int_{\sigma=0}^{t} \int_x \int_y p(x,y,\sigma)\, f(x)\, f(y)\, dx\, dy\; e^{-\frac{C_r}{2M_r}(t-\sigma)} \sin\!\left(\omega_{d_r}(t-\sigma)\right) d\sigma \tag{13}$$

during excitation, and

$$\xi_r(t) = \frac{1}{M_r \omega_{d_r}} \int_{\sigma=0}^{\tau} \int_x \int_y p(x,y,\sigma)\, f(x)\, f(y)\, dx\, dy\; e^{-\frac{C_r}{2M_r}(t-\sigma)} \sin\!\left(\omega_{d_r}(t-\sigma)\right) d\sigma \tag{14}$$

where excitation ceases at time τ.

3.2   Simply – Supported Panel Response to Grazing Incidence Moving Shocks
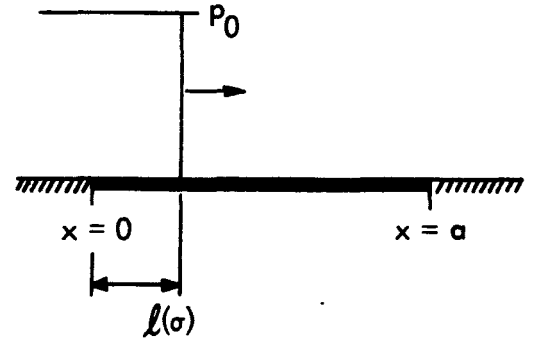
Consider a rectangular panel mounted in an infinite baffle and subjected to a plane step shock of overpressure p_0 moving parallel to a pair of edges, as shown in the above sketch.

If the shock front has reached a position $\ell(\sigma)$ at time σ then the generalized displacement coordinate at time t for the mn^{th} mode is:

$$\xi_{mn}(t) = \frac{1}{M \omega_d} \int_{\sigma=0}^{t} \int_{x=0}^{\ell(\sigma)} \int_{y=0}^{b} p_0\, f(x)\, f(y)\, dx\, dy\; e^{-\frac{C}{2M}(t-\sigma)} \sin\!\left(\omega_d(t-\sigma)\right) d\sigma \tag{15}$$

8

For a simply – supported panel:

$$f(x) = \sin \frac{m\pi x}{a}$$

$$f(y) = \sin \frac{n\pi y}{b}$$

where

$\quad a$ = panel length in x – direction

$\quad b$ = panel width in y – direction

$\quad m$ = mode number (x – direction)

$\quad n$ = mode number (y – direction)

The case of a clamped–clamped panel is discussed in Appendix C.

Thus evaluating Equation (15) for a simply – supported panel gives:

$$\xi_{mn}(t) = \frac{2abp_0}{m\,n\,\pi^2 M\omega_d} \int_{\sigma=0}^{t} [1 - \cos m\pi \, \ell(\sigma)] \, e^{-\frac{C}{2M}(t-\sigma)} \sin\!\left(\omega_d(t-\sigma)\right) d\sigma$$

(if n is an odd integer)

$$\xi_{mn}(t) = 0 \qquad\qquad \text{(if n is an even integer)} \qquad\qquad (16)$$

3.3 Simply – Supported Panel Response to a Grazing Incidence Shock Moving with a Constant Velocity.

3.3.1 Introduction

Before considering the case of a panel subjected to an oscillating shock loading it is instructive to consider the case of a panel which is subjected to a shock which moves across it at constant velocity. This case is not simply one of academic interest, but is of practical interest also. As a space vehicle accelerates through the transonic regime, the shocks which form at the cone-cylinder intersection and at the flares and steps on the vehicle profile tend to run down the structure from one shoulder to the next. The velocity at which these shocks run down the structure is uncertain; Reference 10 suggests approximately 8 in./sec.. However, with a study of the shock patterns formed at different Mach numbers (Reference 11), and a typical Mach number-time curve (Reference 2), a value of 5 ft./sec. would seem more probable. Since these running shocks pass over the vehicle skin, which is not specifically designed to resist oscillating shocks, a running shock could provide a severe loading case for some parts of the vehicle.

3.3.2 Theoretical Analysis

Assume the panel is flat (this is not a severe approximation for panels of large boosters where curvature effects, which raise the natural frequency, are small). Also assume the panel is unstiffened and simply – supported. The case is considered where the panel is initially unloaded and a low pressure region is assumed to move across the panel with a constant velocity in the x – direction as shown in the sketch below.
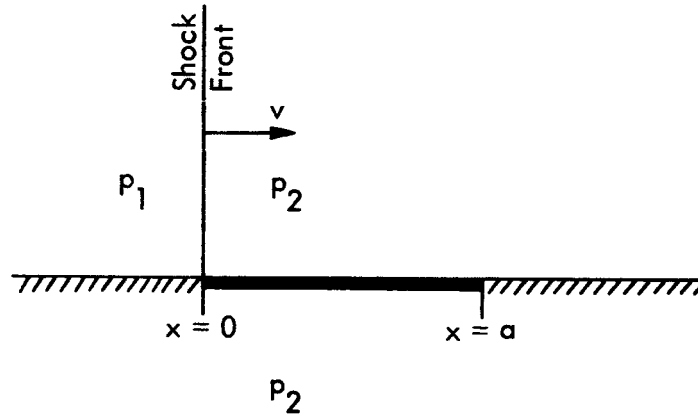
Let $p_2 - p_1 = p_0$, then the pressure at any point x,y on the panel and at time σ may be assumed to be:

$$p(x,y,\sigma) = 0 \qquad\qquad a > x > v\sigma$$

$$p(x,y,\sigma) = p_0 \qquad\qquad v\sigma > x > 0$$

Thus, the panel response is divided into two time regimes (A) and (B). In the analysis which follows, the following symbols $\omega_{d_{mn}}$, $\omega_{0_{mn}}$, M_{mn}, δ_{mn}, and C_{mn} are abbreviated to ω, ω_0, M, δ, and C respectively. Note that $\omega_0^2 = \omega^2 + \left(\dfrac{C}{2M}\right)^2 = \omega^2 + (\omega_0\delta)^2$

(A) <u>For time $0 < t < a/v$</u>: The generalized displacement coordinate of the mn^{th} mode is given by $\xi_{A_{mn}}(t) = \xi_{1_{mn}}(t)$

where:

$$\xi_{1_{mn}}(t) = \frac{1}{M\omega}\int_{\sigma=0}^{t}\int_{x=0}^{v\sigma}\int_{y=0}^{b} p_0 \sin\frac{m\pi x}{a}\sin\frac{n\pi y}{b}\,dx\,dy\,e^{-\omega_0\delta(t-\sigma)}\sin\omega(t-\sigma)d\sigma \qquad (17)$$

The similarity to Equation (15) is immediately noticed as $\ell(\sigma)$ has simply been replaced by $v\sigma$. Thus, using Equation (16), Equation (17) may be shown to be (after integration and rearrangement):

10

$$\xi_{1_{mn}}(t) = \frac{2ab\, P_0}{mn\pi^2 M\omega} \left\{ -\frac{\omega_0\delta \sin\frac{m\pi vt}{a} + (\omega - \frac{m\pi v}{a})\cos\frac{m\pi vt}{a}}{2\left[(\omega_0\delta)^2 + (\omega - \frac{m\pi v}{a})^2\right]} + \right.$$

$$+ \frac{\omega_0\delta \sin\frac{m\pi vt}{a} - (\omega + \frac{m\pi v}{a})\cos\frac{m\pi vt}{a}}{2\left[(\omega_0\delta)^2 + (\omega + \frac{m\pi v}{a})^2\right]} +$$

$$+ \frac{\omega}{\omega_0^2} + e^{-\omega_0\delta t}\left[\frac{\omega_0\delta \sin\omega t + (\omega - \frac{m\pi v}{a})\cos\omega t}{2\left[(\omega_0\delta)^2 + (\omega - \frac{m\pi v}{a})^2\right]} + \right.$$

$$\left.\left. + \frac{\omega_0\delta \sin\omega t + (\omega + \frac{m\pi v}{a})\cdot\cos\omega t}{2\left[(\omega_0\delta)^2 + (\omega + \frac{m\pi v}{a})^2\right]} - \frac{\omega_0\delta \sin\omega t + \omega\cos\omega t}{\omega_0^2}\right]\right\}$$

(where n is an odd integer)

$$\xi_{1_{mn}}(t) = 0, \quad \text{(where m is an even integer).} \tag{18}$$

(B) <u>For time $a/v < t < \infty$:</u> The generalized displacement coordinate of the mn^{th} mode is given by: $\xi_{B_{mn}}(t) = \bar{\xi}_{1_{mn}}(t) + \xi_{2_{mn}}(t)$, where the residual response due to the passage of the shock front across the panel is given by:

$$\bar{\xi}_{1_{mn}}(t) = \frac{1}{M\omega}\int_{\sigma=0}^{\frac{a}{v}}\int_{x=0}^{v\sigma}\int_{y=0}^{b} P_0 \sin\frac{m\pi x}{a}\sin\frac{n\pi y}{b}\, dx\, dy\, e^{-\omega_0\delta(t-\sigma)}\sin\omega(t-\sigma)\, d\sigma \tag{19}$$

which gives on evaluation and much rearrangement:

11

$$\overline{\xi}_{1_{mn}}(t) = \frac{2\,ab\,P_0}{mn\,\pi^2 M\omega}\,e^{-\omega_0\delta t}\left\{e^{\omega_0\delta\frac{a}{v}}\cdot\left[\frac{\omega_0\delta\sin(\frac{\omega a}{v} - \omega t - m\pi) - (\omega - \frac{m\pi v}{a})\cos(\frac{\omega a}{v} - \omega t - m\pi)}{2\left[(\omega_0\delta)^2 + (\omega - \frac{m\pi v}{a})^2\right]} + \right.\right.$$

$$+ \frac{\omega_0\delta\sin(\frac{\omega a}{v} - \omega t + m\pi) - (\omega + \frac{m\pi v}{a})\cos(\frac{\omega a}{v} - \omega t + m\pi)}{2\left[(\omega_0\delta)^2 + (\omega + \frac{m\pi v}{a})^2\right]} - \left.\frac{\omega_0\delta\sin\omega(\frac{a}{v} - t) - \omega\cos\omega(\frac{a}{v} - t)}{\omega_0^2}\right] +$$

$$+ \frac{\omega_0\delta\sin\omega t + (\omega - \frac{m\pi v}{a})\cos\omega t}{2\left[(\omega_0\delta)^2 + (\omega - \frac{m\pi v}{a})^2\right]} + \frac{\omega_0\delta\sin\omega t + (\omega + \frac{m\pi v}{a})\cos\omega t}{2\left[(\omega_0\delta)^2 + (\omega + \frac{m\pi v}{a})^2\right]} - \left.\frac{\omega_0\delta\sin\omega t + \omega\cos\omega t}{\omega_0^2}\right\}$$

(where n is an odd integer),

$$\overline{\xi}_{1_{mn}}(t) = 0 \text{, (where n is an even integer).} \tag{20}$$

The generalized displacement coordinate of the forced response during the second time regime is given by:

$$\xi_{2_{mn}}(t) = \frac{1}{M\omega}\int_{\sigma=a/v}^{t}\int_{x=0}^{a}\int_{y=0}^{b} P_0\sin\frac{m\pi x}{a}\,\sin\frac{n\pi y}{b}\cdot dx\,dy\,e^{-\omega_0\delta(t-\sigma)}\sin\omega(t-\sigma)\,d\sigma \tag{21}$$

which gives on integration and rearrangement:

$$\xi_{2_{mn}}(t) = \frac{4\,ab\,P_0}{mn\,\pi^2 M\omega\omega_0^2}\left\{\omega - e^{\omega_0\delta(\frac{a}{v} - t)}\cdot\left[\omega_0\delta\sin\omega(\frac{a}{v} - t) - \omega\cos\omega(\frac{a}{v} - t)\right]\right\}$$

(where both m and n are odd integers),

$$\xi_{2_{mn}}(t) = 0 \text{, (where either m or n are even integers).} \tag{22}$$

The above integrations were evaluated using commonly tabulated integrals (Reference 12), and the integrals specially evaluated in Reference 13.

3.3.3 Small Damping Case

If damping is negligible then putting $\delta \rightarrow 0$ in Equations (18), (20), and (22), respectively, gives:

$$\xi_{1_{mn}}(t) = \frac{2\,abp_0}{mn\,\pi^2 M}\left[\frac{1 - \cos \omega_0 t}{\omega_0^2} - \frac{\cos \frac{m\pi v t}{a} - \cos \omega_0 t}{\omega_0^2 - \left(\frac{m\pi v}{a}\right)^2}\right]$$

$$\text{(if } n \text{ is an odd integer)}. \tag{23}$$

$$\overline{\xi}_{1_{mn}}(t) = \frac{2\,abp_0}{mn\,\pi^2 M}\left[\frac{\cos \omega_0\left(\frac{a}{v} - t\right) - \cos \omega_0 t}{\omega_0^2} - \frac{\cos\left(\omega_0\frac{a}{v} - \omega_0 t + m\pi\right) - \cos \omega_0 t}{\omega_0^2 - \left(\frac{m\pi v}{a}\right)^2}\right]$$

$$\text{(if } n \text{ is an odd integer)}. \tag{24}$$

$$\xi_{2_{mn}}(t) = \frac{4\,abp_0}{mn\,\pi^2 M\omega_0^2}\left[1 - \cos \omega_0\left(\frac{a}{v} - t\right)\right] \text{(if both } m \text{ and } n \text{ are odd integers)}. \tag{25}$$

again $\xi_{1_{mn}}(t) = \overline{\xi}_{1_{mn}}(t) = 0$, if n is an even integer and $\xi_{2_{mn}}(t) = 0$, if m or n are even integers.

For the case of a shock arriving in a direction normal to the panel surface, $v \rightarrow \infty$, and thus, time regime (A) disappears; $\xi_{1_{mn}}(t)$ and $\overline{\xi}_{1_{mn}}(t)$ must be neglected and the generalized displacement coordinate becomes:

For time $0 < t < \infty$:

$$\xi_{mn}(t) = \frac{4\,abp_0}{mn\,\pi^2 M\omega_0^2}\left[1 - \cos \omega_0 t\right]$$

$$\tag{26}$$

3.3.4. Total Displacement, Strains and Stresses

The total displacement, strains and stresses in the x - and y - directions, respectively, of any point on the panel, may be determined by substituting the appropriate value of $\xi_{A_{mn}}(t)$ or $\xi_{B_{mn}}(t)$ and the values of x and y into Equations (4), (5), and (6) and then (7) and (8).

3.3.5 Displacement of Panel for Large Time

It is interesting to note that the deflection of a uniform simply - supported panel, subjected to a uniform pressure p_0 (see Reference 8, p. 110), may be written (when the symbols are rationalized):

$$G(x,y,t) = \frac{16 p_0}{\pi^6} \cdot \frac{12(1-\nu^2)}{E h^3} \sum_{m=1}^{\infty} \sum_{n=1}^{\infty} \frac{\sin\frac{m\pi x}{a} \sin\frac{n\pi y}{b}}{mn\left[\frac{m^2}{a^2} + \frac{n^2}{b^2}\right]^2} \tag{27}$$

(where m and n are odd integers).

but for a simply - supported panel:

$$\omega_{0_{mn}} = \pi^2 h \left[\frac{m^2}{a^2} + \frac{n^2}{b^2}\right]\sqrt{\frac{E}{12\,\rho(1-\nu^2)}} \tag{28}$$

and:

$$M_{mn} = \rho\, h\, a\, b/4 \tag{29}$$

Thus, Equation (27) may be rewritten:

$$G(x,y,t) = \frac{4 p_0\, ab}{\pi^2} \sum_{m=1}^{\infty} \sum_{n=1}^{\infty} \frac{\sin\frac{m\pi x}{a} \sin\frac{n\pi y}{b}}{mn\, m\, \omega_{0_{mn}}^2} \tag{30}$$

Some time after the panel is subjected to a step shock wave, if it is viscously damped, the panel vibrations will decay and the displacement of the panel should be equal to that of a panel subjected to a uniform pressure p_0. Thus, if $t \rightarrow \infty$ in time regime (B) above in Section 3.3.2, the displacement should be equivalent to that given by Equation (30). Putting $t \rightarrow \infty$, it is seen that $\xi_{1_{mn}}(t) \rightarrow 0$

$\left[\text{from Equation (20)}\right]$ and $\xi_{2_{mn}}(t) \rightarrow \dfrac{4\, abp_0}{mn\, \pi^2 M \omega_0^2}$ (where both m and n are odd integers).

Thus, the total displacement is given by Equation (4):

14

$$G(x,y,t) = \sum_{m=1}^{\infty} \sum_{n=1}^{\infty} \left[\frac{4\,ab\,P_0}{mn\,\pi^2 M\omega_0^2} \sin\frac{m\pi x}{a} \sin\frac{n\pi y}{b} \right] \tag{31}$$

It is seen that Equations (30) and (31) are identical and that the panel equilibrium displacement after a long time is that due to the uniform pressure P_0.

3.4 Simply – Supported Viscously Damped Panel Response to Grazing Incidence Sinusoidally Oscillating Shocks

Assume the position of the shock front at time σ is given by Equation (2):

$$x = D + H \sin \alpha \sigma \tag{2}$$

Putting $\ell(\sigma) = D + H \sin \alpha\sigma$ in Equation (16), thus gives the generalized displacement coordinate of the mn^{th} mode for panel response to the sinusoidally oscillating shock:

$$\xi_{mn}(t) = \frac{2\,ab\,P_0}{mn\,\pi^2 M\omega} \int_{\sigma=0}^{t} \left[1 - \cos\left(\frac{m\pi D}{a} + \frac{m\pi H}{a}\sin \alpha\sigma\right) \right] e^{-\omega_0\delta(t-\sigma)} \sin \omega(t-\sigma)d\sigma \tag{32}$$

However, Equation (32) includes the effect of a suddenly applied pressure over the panel from $x = 0$ to $x = D$, the generalized displacement coordinate of which is given by:

$$\xi_{static_{mn}}(t) = \frac{2\,ab\,P_0}{mn\,\pi^2 M\omega} \int_{0}^{t} \left(1 - \cos\frac{m\pi D}{a}\right) e^{-\omega_0\delta(t-\sigma)} \sin \omega(t-\sigma)\, d\sigma \tag{33}$$

Thus, the panel vibrations due only to the shock oscillations are given by Equation (32) less Equation (33):

$$\xi_{osc_{mn}}(t) = \frac{2\,ab\,P_0}{mn\,\pi^2 M\omega} \int_{0}^{t} \left[\cos\frac{m\pi D}{a} - \cos\left(\frac{m\pi D}{a} + \frac{m\pi H}{a}\sin \alpha\sigma\right) \right] e^{-\omega_0\delta(t-\sigma)} \sin \omega(t-\sigma)d\sigma \tag{34}$$

This method used is similar to that used by Ungar in Reference 14, with the exception that viscous damping is included from the beginning of the analysis, while in Reference 14 damping is not included and suggestions are simply made for its inclusion when the analysis is completed.

15

Expanding the second term, Equation (34) becomes:

$$\xi_{osc_{mn}}(t) = \frac{2\,ab\,P_0}{mn\,\pi^2\,M\omega}\int_0^t \left[\cos\frac{m\pi D}{a} - \left(\cos\frac{m\pi D}{a}\right)\cos(\frac{m\pi H}{a}\sin\alpha\sigma) + \right.$$

$$\left. + \left(\sin\frac{m\pi D}{a}\right)\sin\left(\frac{m\pi H}{a}\cdot\sin\alpha\sigma\right)\right] e^{-\omega_0\delta(t-\sigma)}\sin\omega(t-\sigma)\,d\sigma \tag{35}$$

Integrating the first term in the above equation is straightforward; however, obtaining a closed form solution for the integrals of the second and third terms does not appear possible. In this section of the report, an approximation is made for the second and third terms which is only valid if $m\pi H/a$ is small. A much better approximation (using Bessel functions) which does not restrict the maximum value of $m\pi H/a$ is given in Appendix B.

Putting $m\pi H/a = \mu$ and $\alpha\sigma = z$ and using only the first term in the series expansion for sine, which is thus valid only when μ is small gives:

$$\sin(\mu\sin z) \approx \mu\sin z \approx \sin\mu\sin z \tag{36}$$

Using only the first two terms in the series expansion for cosine, which again is only valid for small μ gives:

$$\cos(\mu\sin z) \approx 1 - \frac{1}{2}(\mu\sin z)^2 \approx 1 - 2\sin^2\frac{\mu}{2}\sin^2 z$$

$$\approx 1 - \frac{1}{2}(1 - \cos\mu)(1 - \cos 2z)$$

$$\cos(\mu\sin z) \approx \frac{1}{2}(1 + \cos\mu) + \frac{1}{2}(1 - \cos\mu)\cdot\cos 2z \tag{37}$$

Figure 2 (extracted from Reference 14) shows the accuracy of these approximations for two different values of μ. As expected, the approximations are better for small values of μ, and $\mu = \pi/2$ would seem to be the largest reasonably acceptable value which should be used.

Substituting these approximations into Equation (35) gives:

$$\xi_{osc_{mn}}(t) \approx \frac{2\,ab\,P_0}{mn\,\pi^2\,M\omega}\int_0^t \left[\frac{1}{2}(\cos\frac{m\pi D}{a})(1 - \cos\frac{m\pi D}{a}) - \frac{1}{2}(\cos\frac{m\pi D}{a})(1 - \cos\frac{m\pi H}{a})\cos 2\alpha\sigma + \right.$$

$$\left. + \sin\frac{m\pi D}{a}\sin\frac{m\pi H}{a}\sin\alpha\sigma\right] e^{-\omega_0\delta(t-\sigma)}\sin\omega(t-\sigma)\,d\sigma$$

(provided n is an odd integer and $\frac{m\pi H}{a}$ is small). (38)

16

Equation (38) contains three terms which are integrated separately:

$$I_1 = -\frac{2\,ab\,P_0}{mn\,\pi^2\,M\omega}\int_0^t \frac{1}{2}(\cos\frac{m\pi D}{a})(1 - \cos\frac{m\pi H}{a})\,e^{\omega_0\delta(\sigma-t)}\sin\omega(\sigma-t)\,d\sigma \tag{39}$$

which gives on evaluation:

$$I_1 = \frac{ab\,P_0}{mn\,\pi^2\,M\omega\omega_0^2}(\cos\frac{m\pi D}{a})(1 - \cos\frac{m\pi H}{a})\left[\omega - e^{-\omega_0\delta t}\left[\omega_0\delta\sin\omega t + \omega\cos\omega t\right]\right] \tag{40}$$

$$I_2 = \frac{ab\,P_0}{mn\,\pi^2\,M\omega}\int_0^t (\cos\frac{m\pi D}{a})(1 - \cos\frac{m\pi H}{a})\,e^{\omega_0\delta(\sigma-t)}\sin\omega(\sigma-t)\cos 2\alpha\sigma\,d\sigma \tag{41}$$

which gives on evaluation:

$$I_2 = \frac{ab\,P_0}{mn\,\pi^2\,M\omega}(\cos\frac{m\pi D}{a})(1 - \cos\frac{m\pi H}{a})\bullet$$

$$\bullet\left[-\frac{\omega_0\delta\sin 2\alpha t + (\omega - 2\alpha)\bullet\cos 2\alpha t - e^{-\omega_0\delta t}\left[\omega_0\delta\sin\omega t + (\omega-2\alpha)\bullet\cos\omega t\right]}{2\left[(\omega_0\delta)^2 + (\omega - 2\alpha)^2\right]}\right.+$$

$$\left.+\frac{\omega_0\delta\sin 2\alpha t - (\omega + 2\alpha)\bullet\cos 2\alpha t + e^{-\omega_0\delta t}\left[\omega_0\delta\sin\omega t + (\omega + 2\alpha)\bullet\cos\omega t\right]}{2\left[(\omega_0\delta)^2 + (\omega + 2\alpha)^2\right]}\right] \tag{42}$$

and,

$$I_3 = -\frac{2\,ab\,P_0}{mn\,\pi^2\,M\omega}(\sin\frac{m\pi D}{a})(\sin\frac{m\pi H}{a})\int_0^t e^{\omega_0\delta(\sigma-t)}\sin\omega(\sigma-t)\sin\alpha\sigma\,d\sigma \tag{43}$$

which gives on evaluation:

$$I_3 = \frac{2\,ab\,P_0}{mn\,\pi^2 M\omega}(\sin\frac{m\pi D}{a})(\sin\frac{m\pi H}{a})\left[\frac{(\omega-\alpha)\sin\alpha t - \omega_0\delta\cos\alpha t - e^{-\omega_0\delta t}\left[(\omega-\alpha)\sin\omega t - \omega_0\delta\cos\omega t\right]}{2\left[(\omega_0\delta)^2 + (\omega-\alpha)^2\right]}\right.$$

$$\left. + \frac{(\omega+\alpha)\sin\alpha t + \omega_0\delta\cos\alpha t + e^{-\omega_0\delta t}\left[(\omega+\alpha)\sin\omega t - \omega_0\delta\cos\omega t\right]}{2\left[(\omega_0\delta)^2 + (\omega+\alpha)^2\right]}\right] \tag{44}$$

Thus:

$$\xi_{osc_{mn}}(t) = \frac{ab\,P_0}{mn\,\pi^2 M\omega^2}\left\{(\cos\frac{m\pi D}{a})(1-\cos\frac{m\pi H}{a})\left\{\left(\frac{\omega}{\omega_0}\right)^2 - e^{-\omega_0\delta t}\left[\frac{\omega}{\omega_0}\delta\sin\omega t + \left(\frac{\omega}{\omega_0}\right)^2\cdot\cos\omega t\right]\right.\right. -$$

$$- \frac{\omega}{2}\left[\frac{\omega_0\delta\sin 2\alpha t + (\omega-2\alpha)\cos 2\alpha t - e^{-\omega_0\delta t}\left[\omega_0\delta\sin\omega t + (\omega-2\alpha)\cos\omega t\right]}{(\omega_0\delta)^2 + (\omega-2\alpha)^2}\right] -$$

$$\left.\left. - \frac{\omega_0\delta\sin 2\alpha t + (\omega+2\alpha)\cos 2\alpha t + e^{-\omega_0\delta t}\left[\omega_0\delta\sin\omega t + (\omega+2\alpha)\cos\omega t\right]}{(\omega_0\delta)^2 + (\omega+2\alpha)^2}\right]\right\} +$$

$$+ (\sin\frac{m\pi D}{a})(\sin\frac{m\pi H}{a})\left\{\frac{(\omega-\alpha)\sin\alpha t - \omega_0\delta\cos\alpha t - e^{-\omega_0\delta t}\left[(\omega-\alpha)\sin\omega t - \omega_0\delta\cos\omega t\right]}{(\omega_0\delta)^2 + (\omega-\alpha)^2}\right. +$$

$$\left.\left. + \frac{(\omega+\alpha)\sin\alpha t + \omega_0\delta\cos\alpha t + e^{-\omega_0\delta t}\left[(\omega+\alpha)\sin\omega t - \omega_0\delta\cos\omega t\right]}{(\omega_0\delta)^2 + (\omega+\alpha)^2}\right\}\right\} \tag{45}$$

If damping is small, $\delta \to 0$ and Equation (45) reduces to:

$$\xi_{osc_{mn}}(t) = \frac{ab\,P_0}{mn\,\pi^2 M\omega_0^2}\left\{(\cos\frac{m\pi D}{a})(1-\cos\frac{m\pi H}{a})\left\{1 - \cos\omega_0 t - \omega_0^2\left[\frac{\cos 2\alpha t - \cos\omega_0 t}{\omega_0^2 - (2\alpha)^2}\right]\right\} +$$

$$+ 2\omega_0(\sin\frac{m\pi D}{a})(\sin\frac{m\pi H}{a})\cdot\left[\frac{\omega_0\sin\alpha t - \alpha\cdot\sin\omega_0 t}{\omega_0^2 - \alpha^2}\right]\right\} \tag{46}$$

18

which agrees with the result obtained by Ungar in Reference 14, except that the term in this analysis, with $\omega^2 - (2\alpha)^2$ as the denominator, is half the value of the equivalent term in the analysis of Reference 14, which is believed to be in error.

For large time, $t \rightarrow \infty$, Equation (45) reduces to:

$$
\xi_{osc_{mn}}(t) = \frac{ab \, P_0}{mn \, \pi^2 M \omega^2} \Bigg\{ (\cos \frac{m\pi D}{a}) \cdot (1 - \cos \frac{m\pi H}{a}) \Bigg\{ \left(\frac{\omega}{\omega_0}\right)^2 - \frac{\omega}{2} \Bigg[\frac{\omega_0 \delta \sin 2\alpha t + (\omega - 2\alpha) \cdot \cos 2\alpha t}{(\omega_0 \delta)^2 + (\omega - 2\alpha)^2} -
$$

$$
- \frac{\omega_0 \delta \sin 2\alpha t - (\omega + 2\alpha) \cdot \cos 2\alpha t}{(\omega_0 \delta)^2 + (\omega + 2\alpha)^2} \Bigg] \Bigg\} + \omega (\sin \frac{m\pi D}{a})(\sin \frac{m\pi H}{a}) \cdot \Bigg\{ \frac{(\omega - \alpha) \cdot \sin \alpha t - \omega_0 \delta \cos \alpha t}{(\omega_0 \delta)^2 + (\omega - \alpha)^2} +
$$

$$
+ \frac{(\omega + \alpha) \cdot \sin \alpha t + \omega_0 \delta \cos \alpha t}{(\omega_0 \delta)^2 + (\omega + \alpha)^2} \Bigg\} \Bigg\}
$$

(47)

4.0 DISCUSSION AND COMPUTATION OF RESULTS

It must be remembered that Equations (45),(46), and (47) are approximate only and are only valid for small amplitude shock oscillations and it is recommended that they are not used for $H > a/2m$. However, it is observed that all three equations show that $\xi_{osc_{mn}}(t)$ vanishes for $H \to 0$, the expected result. $\xi_{osc_{mn}}(t)$ also vanishes for $H = 2 \lambda a/m$, where λ is any integer; however, this result is of little practical interest since the equations are only valid for $H < a/2m$.

It is observed that Equation (47) indicates that for a damped panel, after a large time when steady state oscillations are reached, the vibrations are composed only of vibrations at the forcing frequency, the free or natural frequency vibrations having subsided to zero. This is a general result for harmonically forced vibrations (see Reference 9, p. 39 et seq.).

It is observed from all three equations that there are panel resonances when $\alpha \to \omega/2$ and when $\alpha \to \omega$.

4.1 First Mode Response to Shock Oscillating About Panel Center

If $D = a/2$, $(m = 1)$, for $\alpha \to \omega$; Equation (47) reduces to:

$$\xi_{osc_{mn}}(t) = \frac{ab\,P_0}{mn\,\pi^2 M\omega^2}\left(\sin\left(\frac{\pi H}{a}\right)\right)\left\{-\frac{\cos\alpha t}{\delta} + \frac{\omega_0(2\omega\sin\alpha t + \omega_0\delta\cos\alpha t)}{(\omega_0\delta)^2 + (2\omega)^2}\right\}$$

(48)

If $\delta \to 0$, Equation (48) reduces to (since $\omega \to \omega_0$):

$$\xi_{osc}(t) \approx \frac{ab\,P_0}{mn\,\pi^2 M\omega_0^2}\left(\sin\left(\frac{\pi H}{a}\right)\right)\left\{-\frac{\cos\alpha t}{\delta} + \frac{2\sin\alpha t + \delta\cos\alpha t}{\delta^2 + 4}\right\}$$

(49)

but if $\delta \to 0$

$$\xi_{osc_{mn}}(t) \approx \frac{ab\,P_0}{mn\,\pi^2 M\omega_0^2}\left\{\left(\sin\frac{\pi H}{a}\right)\left[-\frac{\cos\alpha t}{\delta}\right]\right\}$$

(50)

Figure 3 shows the dynamic magnification factor (for the first mode) plotted against the amplitude of shock oscillation for different values of the panel damping ratio δ. The amplification factor was obtained by dividing the maximum value of Equation (50) by the first term of Equation (31). It should be noted that although this plot is for the first mode dynamic magnification factor, it is also approximately correct for the overall

20

dynamic magnification factor, because the higher mode displacements are very small compared with that of the first mode.

4.2 First Mode Response to Shock Oscillating About Panel Edge

For $D = 0$, $(m = 1)$ and $a/2 \rightarrow \omega$, Equation (47) reduces to:

$$\xi_{osc_{mn}}(t) = \frac{ab\,P_0}{mn\,\pi^2 M\omega^2} \left\{ \left[1 - \cos\left(\frac{\pi H}{a}\right)\right] \left[\left(\frac{\omega}{\omega_0}\right)^2 - \frac{\omega}{2\omega_0\delta}\sin 2\alpha t - \frac{\omega\omega_0\delta \sin 2\alpha t - 5\omega^2 \cdot \cos^2 \alpha t}{2\left[(\omega_0\delta)^2 + 25\omega^2\right]}\right] \right\} \quad (51)$$

but if δ is small then $\omega \rightarrow \omega_0$ and Equation (51) becomes:

$$\xi_{osc_{mn}}(t) \approx \frac{ab\,P_0}{mn\,\pi^2 M\omega^2} \left\{ \left[1 - \cos\left(\frac{\pi H}{a}\right)\right] \left[1 - \frac{\sin 2\alpha t}{2\delta} - \frac{\delta \sin 2\alpha t - 5 \cos 2\alpha t}{2\delta^2 + 50}\right] \right\} \quad (52)$$

but if $\delta \rightarrow 0$

$$\xi_{osc_{mn}}(t) \approx \frac{ab\,P_0}{mn\,\pi^2 M\omega^2} \left\{ \left[1 - \cos\left(\frac{\pi H}{a}\right)\right] \left[1 - \frac{\sin 2\alpha t}{2\delta}\right] \right\} \quad (53)$$

Figure 4 shows the dynamic magnification factor (for the first mode) plotted against amplitude of shock oscillation for different values of the panel damping ratio δ. The amplification factor was obtained by dividing the maximum value of Equation (53) by the first term of Equation (31). Again it should be noted that although this plot is for the first mode dynamic magnification factor, it is also approximately correct for the overall dynamic magnification factor, because the higher mode displacements are small compared with the first mode.

4.3 Analysis of Results Computed by the Digital Computer Program

As discussed in Appendix D, Equation (47) was programmed for analysis by a digital computer. Figure 5 shows two typical plots of first mode response divided by response to the same static load against non-dimensionalized time for two forcing frequencies near to the two resonances. A representative value of damping ratio δ is chosen. Figure 6 shows a plot of the dynamic amplification factor for the first mode as a function of shock amplitude for the shock oscillating about the panel center. The different plots in this figure indicate how moving the forcing frequency slightly off the resonant frequency reduces the amplification factor; a 5% increase in frequency is sufficient to reduce the dynamic magnification factor by a factor of 10. In Figure 7, the data of Figure 6 is replotted in the form of a typical displacement versus frequency resonance curve.

21

In Figures 8 and 9 typical plots of dynamic amplication factor against non-dimensionalized frequency are also given for shock oscillations about a position of $D/a = 0.2$. The different plots on each curve are for different shock oscillation amplitudes. The two Figures 8 and 9 are for the first resonance ($a/\omega = 0.5$) and the second resonance ($a/\omega = 1.0$) respectively. It is observed that the dynamic magnification factor is much more dependent upon the shock oscillation amplitude for the first resonance than for the second. Figures 7, 8 and 9 are all plotted for damping ratio $\delta = 0.005$. The damping ratio for typical structures is in the range of $\delta = 0.005$ to 0.02, so this is a realistic value of δ to choose.

Figures 10 and 11 show plots of the dynamic magnification factor against mean position of the oscillating shock (X/a) for three representative values of δ and for shock frequencies of $\beta = 0.5$ and 1.0. In Figure 10 the dynamic magnification factor is given for shock oscillations of amplitude ($H/a = 0.1$); in Figure 11 the shock oscillation amplitude is $H/a = 0.5$. In recent tests in the 7 inch supersonic tunnel at the Marshall Space Flight Center, Huntsville, Alabama, shock waves have been observed to oscillate during steady tunnel runs at a Mach number $M = 2.44$. The excursions of the shock waves were of the order of a boundary layer thickness. Scaling this oscillation to the Saturn V and panels near to the flare would suggest that $H/a \approx 0.1$ is a reasonable value. Thus the dynamic magnification factor given in Figure 10 would seem to be realistic provided the shock couples to the first resonant frequencies of the local panels.

5.0   CONCLUSIONS

The experimental data of oscillating shock loads experienced by space vehicles which were examined were inconclusive. There is evidence to show that shocks can oscillate at discrete frequencies and also in a random manner. The case of a shock oscillating at a discrete frequency received principal attention. An approximate analysis was formulated and some numerical evaluation of the theoretical results undertaken. It is shown that amplification factors of up to 50 can be experienced by a panel with a damping ratio of about 0.005; this factor decreases to 12.5 for a damping ratio of 0.02. This factor is for the first mode for a shock oscillating at the panel resonant frequency about the middle point of the panel with an amplitude of the semi-span; this appears to be the worst case. It is suggested that for the Saturn V a more realistic dynamic magnification factor would be between 5 and 15 (see Figure 10); this assumes a shock oscillating about the center of a typical panel at the panel resonant frequency and panel damping ratios of between 0.005 and 0.02.

An analysis in Appendix A gives a method of determining panel response to shocks oscillating at constant speed. The case of shocks running down the vehicle is also considered in this report. A much more exact solution for the case of sinusoidally oscillating shocks is given in Appendix B. In this analysis no restriction is placed on the shock oscillation amplitude. This more refined analysis also shows that resonance will occur in each mode of the panel if it is subjected to shocks oscillating with any "sub-harmonic" (i.e., ω, $\omega/2$, $\omega/3$, $\omega/4$, etc.) of the natural damped resonant frequency of the panel.

Most of the analyses in this report are restricted to simply-supported panels with viscous damping; however, in Appendix C a method is given which shows how the analyses can be extended to clamped-clamped panels to a good engineering approximation.

The reader is referred to References 15, 16 and 17 for theoretical and experimental analyses of panel response to traveling sonic boom (N - waves), explosive blast and to step shock waves.

6.0 RECOMMENDATIONS

It is suggested that the theoretical analysis of Appendix B, which has no restriction placed on shock oscillation amplitude, deserves further attention and digital computation. This analysis should give accurate answers for the larger shock amplitudes and also for the panel response in its higher modes which cannot be attempted with the approximate analysis.

7.0   ACKNOWLEDGEMENTS

APPENDIX A

SOLUTION OF PANEL RESPONSE TO OSCILLATING SHOCKS BY THE SUMMATION OF INTEGRALS

As is discussed in the Introduction and Section 2 of this report, the manner of oscillation of shock waves relative to space vehicles is not at all well defined. Also, if the velocity of oscillation of the shock becomes comparable to that of the vehicle, the pressure downstream of the shock will be different when the shock moves upstream from when it moves downstream. The analysis which follows shows how the analysis of Section 3.3 can be developed to allow for these factors.

1. **Simply Supported Panel Response to a Step Shock Oscillating at a Constant Speed**

(a) Consider the case of a flat panel, initially unloaded, which is then subjected to a pressure step p_0 which sweeps from $x = 0$ to $x = a$ and back repeatedly at constant speed v.

The panel response is divided into time regimes which encompass each sweep of the shock front across the panel.

Then:

(A) For time $0 < t < a/v$ $\qquad \xi_A = \xi_1$

(B) For time $a/v < t < 2a/v$ $\qquad \xi_B = \bar{\xi}_1 + \xi_2 + \xi_3$

(C) For time $2a/v < t < 3a/v$ $\qquad \xi_C = \bar{\xi}_1 + \xi_2 + \bar{\xi}_3 + \xi_4 + \xi_5$

etc.,

where ξ_{mn} has been abbreviated to ξ, the generalized displacement co-ordinate of the mn^{th} mode, and is given by:

$$\xi_{1_{mn}}(t) = \int_{\sigma=0}^{t} \int_{x=0}^{v\sigma} \int_{y=0}^{b} \left[p_0 \cdot F(x,y,\sigma) \right] dx\, dy\, d\sigma$$

$$\bar{\xi}_{1_{mn}}(t) = \int_{\sigma=0}^{a/v} \int_{x=0}^{v\sigma} \int_{y=0}^{b} \left[p_0 \cdot F(x,y,\sigma) \right] dx\, dy\, d\sigma \qquad\qquad (A1)$$

$$\xi_{2_{mn}}(t) = \int_{\sigma=a/v}^{t} \int_{x=0}^{a} \int_{y=0}^{b} \left[p_0 \cdot F(x,y,\sigma) \right] dx\, dy\, d\sigma$$

26

$$\xi_{3_{mn}}(t) = \int_{\sigma=a/v}^{t} \int_{x=2a-v\sigma}^{a} \int_{y=0}^{b} \left[-p_0 \cdot F(x,y,\sigma) \right] dx\, dy\, d\sigma$$

$$\overline{\xi_{3_{mn}}}(t) = \int_{\sigma=a/v}^{2a/v} \int_{x=2a-v\sigma}^{a} \int_{y=0}^{b} \left[-p_0 \cdot F(x,y,\sigma) \right] dx\, dy\, d\sigma$$

$$\xi_{4_{mn}}(t) = \int_{\sigma=2a/v}^{t} \int_{x=0}^{a} \int_{y=0}^{b} \left[-p_0 \cdot F(x,y,\sigma) \right] dx\, dy\, d\sigma$$

$$\xi_{5_{mn}}(t) = \int_{\sigma=2a/v}^{t} \int_{x=0}^{2a-v\sigma} \int_{y=0}^{b} \left[p_0 \cdot F(x,y,\sigma) \right] dx\, dy\, d\sigma$$

(A1)

where $F(x,y,\sigma) = \sin\dfrac{m\pi x}{a} \sin\dfrac{n\pi y}{b}\; e^{-\omega_0\delta(t-\sigma)} \dfrac{\sin\omega(t-\sigma)}{M\omega}$

It is seen that the integrals $\xi_{1_{mn}}(t)$, $\overline{\xi}_{1_{mn}}(t)$ and $\xi_{2_{mn}}(t)$ have already been evaluated in Section 3.3 of this report. Some simplification may be achieved in the later time regimes by summing some of the integrals. For instance in time regime (C):

$$\xi_{2_{mn}}(t) + \xi_{4_{mn}}(t) = \int_{\sigma=a/v}^{2a/v} \int_{x=0}^{a} \int_{y=0}^{b} \left[p_0 F(x,y,\sigma) \right] dx\, dy\, d\sigma$$

However, probably the simplest way to evaluate the panel response after it has been subjected to several crossings of the shock is to evaluate the general integral:

$$\xi_{mn}(t) = \int_{\sigma=Sa/v}^{Tt+Ua/v} \int_{x=Wa+Xv\sigma}^{Ya+Zv\sigma} \int_{y=0}^{b} \left[p_0 \cdot F(x,y,\sigma) \right] dx\, dy\, d\sigma$$

(A2)

where S, T, U, W, X, Y, and Z are integers.

This method of determining panel response may appear to be lengthy; however, with the use of Equation (A2) and a digital computer, it should not be impracticable. It should be noted that this method is sufficiently flexible to allow the use of a different value of p_0 and v as the shock moves up and downstream, if this refinement is required.

(b)   The panel response is also readily formulated if the shock does not oscillate completely across the panel but about some mean position D.   The integrations are now made between $x = D - H$ and $x = D + H$ where 2H is the shock front excursion, instead of between $x = 0$ and $x = a$.   For instance, the first three integrals of Equations (A1) above $\xi_{1_{mn}}(t)$, $\bar{\xi}_{1_{mn}}(t)$, and $\xi_{2_{mn}}(t)$ would now become:

$$\xi_{1_{mn}}(t) = \int_{\sigma=0}^{t} \int_{x=D}^{v\sigma} \int_{y=0}^{b} \left[P_0 \cdot F(x,y,\sigma) \right] dx\, dy\, d\sigma$$

$$\bar{\xi}_{1_{mn}}(t) = \int_{\sigma=0}^{H/v} \int_{x=D}^{v\sigma} \int_{y=0}^{b} \left[P_0 \cdot F(x,y,\sigma) \right] dx\, dy\, d\sigma \qquad \left.\vphantom{\int_0^t}\right\} \text{(A3)}$$

$$\xi_{2_{mn}}(t) = \int_{\sigma=H/v}^{t} \int_{x=D}^{D+H} \int_{y=0}^{b} \left[P_0\, F(x,y,\sigma) \right] dx\, dy\, d\sigma$$

if the shock is assumed to start oscillating about the mean position D.

2.   <u>Simply – Supported Panel Response to a Sinusoidally Oscillating Step Shock</u>

The integrals are again formulated in a similar manner to those in Equations (A1) and (A3) above. Again the integrations are made between $x = D - H$ and $x = D + H$. The distance $v\sigma$ now becomes $H \sin\alpha\sigma$ if α is the angular frequency of oscillation. The time H/v now becomes $\pi/2\alpha$ if the shock front is assumed to start oscillating about a mean position D. The first three integrals $\xi_{1_{mn}}(t)$, $\bar{\xi}_{1_{mn}}(t)$, and $\xi_{2_{mn}}(t)$ would now become:

$$\xi_{1_{mn}}(t) = \int_{\sigma=0}^{t} \int_{x=D}^{H \sin\alpha\sigma} \int_{y=0}^{b} \left[P_0 \cdot F(x,y,\sigma) \right] dx\, dy\, d\sigma$$

$$\bar{\xi}_{1_{mn}}(t) = \int_{\sigma=0}^{\pi/2\alpha} \int_{x=D}^{H \sin\alpha\sigma} \int_{y=0}^{b} \left[P_0 \cdot F(x,y,\sigma) \right] dx\, dy\, d\sigma \qquad \left.\vphantom{\int_0^t}\right\} \text{(A4)}$$

$$\xi_{2_{mn}}(t) = \int_{\sigma=0}^{t} \int_{x=D}^{H} \int_{y=0}^{b} \left[P_0\, F(x,y,\sigma) \right] dx\, dy\, d\sigma$$

28

This method proposed is alternative to that developed in Section 3.4 of the report.

For each analysis developed in this Appendix, the total displacement, strains and stresses in the x – and y – directions, respectively, of any point on the panel may be determined by substituting the appropriate value of the generalized displacement $\xi_{mn}(t)$ and values of x and y into Equations (4), (5), (6), (7), and (8) respectively.

APPENDIX B

SOLUTION OF PANEL RESPONSE TO SINUSOIDALLY OSCILLATING SHOCKS BY THE USE OF BESSEL FUNCTIONS

In Section 3.4 of this report, approximations for the functions $\cos\left(\frac{m\pi H}{a}\sin\alpha\sigma\right)$ and $\sin\left(\frac{m\pi H}{a}\sin\alpha\sigma\right)$ are made using Equations (36) and (37). This allows the integration of Equation (35) to be made, although in practice it restricts the oscillating shock to small amplitudes relative to the panel span, particularly for the case of the higher modes.

However, it is noted that the use of Bessel functions allows a series solution to be found for the above functions and thus a much more accurate analysis for panel response to oscillating shocks can be formulated which is no longer restricted in the amplitude of oscillation of the shock front.

Reference 18 gives:

$$\sin(\mu \sin z) = 2\sum_{k=0}^{\infty}\left[\frac{J_{2k+1}(\mu)}{}\sin\left[(2k+1)z\right]\right]$$
(B1)

$$\cos(\mu \sin z) = J_0(\mu) + 2\sum_{k=1}^{\infty}\left[J_{2k}(\mu)\cos\left[2kz\right]\right]$$
(B2)

where:

J_0 is a Bessel Function of the First kind, zero order,

J_{2k} is a Bessel Function of the First kind, $2k^{th}$ order,

J_{2k+1} is a Bessel Function of the First kind, $(2k+1)^{th}$ order.

These two identities $\left[\text{Equations (B1) and (B2)}\right]$ may be compared with Equations (36) and (37). Substituting these identities into Equation (35) gives:

$$\xi_{osc_{mn}} = \frac{2ab\,P_0}{mn\,\pi^2\,M\omega}\int_0^t\left\{\cos\frac{m\pi D}{a} - \left(\cos\frac{m\pi D}{a}\right)\cdot\left[J_0\left(\frac{m\pi H}{a}\right) + 2\sum_{k=1}^{\infty}\left[\left(J_{2k}\left(\frac{m\pi H}{a}\right)\right)\cos(2k\alpha\sigma)\right]\right]\right.$$

$$\left. + 2\sin\frac{m\pi D}{a}\sum_{k=0}^{\infty}\left[\left(J_{2k+1}\left(\frac{m\pi H}{a}\right)\right)\sin((2k+1)\alpha\sigma)\right]\right\}e^{-\omega_0\delta(t-\sigma)}\sin\omega(t-\sigma)\,d\sigma$$
(B3)

(provided n is an odd integer)

$\xi_{osc_{mn}} = 0$ (if n is an even integer).

30

The equation may be separated into three integrals which are evaluated separately:

$$I_1 = -\frac{2\,ab\,P_0}{mn\,\pi^2 M\omega} \cdot (\cos\frac{m\pi D}{a})\left[1 - J_0\left(\frac{m\pi H}{a}\right)\right] \int_0^t e^{\omega_0\delta(\sigma-t)} \sin\omega(\sigma-t)\,d\sigma \tag{B4}$$

$$I_1 = \frac{2\,ab\,P_0}{mn\,\pi^2 M\omega\omega_0^2} \cdot (\cos\frac{m\pi D}{a})\cdot\left[1 - J_0\left(\frac{m\pi H}{a}\right)\right]\left[\omega - e^{-\omega_0\delta t}(\omega_0\delta\sin\omega t + \omega\cos\omega t)\right] \tag{B5}$$

$$I_2 = \frac{4\,ab\,P_0}{mn\,\pi^2 M\omega} \cdot (\cos\frac{m\pi D}{a}) \cdot \int_{\sigma=0}^t \sum_{k=1}^\infty \left[\left[J_{2k}\left(\frac{m\pi H}{a}\right)\right]e^{\omega_0\delta(\sigma-t)} \sin(\omega(\sigma-t))\cos(2k\alpha\,\sigma)\,d\sigma\right] \tag{B6}$$

$$I_2 = \frac{4\,ab\,P_0}{mn\,\pi^2 M\omega}(\cos\frac{m\pi D}{a}) \left\{ \sum_{k=1}^\infty \left[\left[J_{2k}\left(\frac{m\pi H}{a}\right)\right]\left[\right.\right.\right.$$

$$-\frac{\omega_0\delta\sin(2k\alpha t)+(\omega-2k\alpha)\cdot\cos(2k\alpha\,t)- e^{-\omega_0\delta t}\left[\omega_0\delta\sin\omega t + (\omega-2k\alpha)\cdot\cos\omega t\right]}{2\left[(\omega_0\delta)^2 + (\omega-2k\alpha)^2\right]} +$$

$$+\frac{\omega_0\delta\sin(2k\alpha\,t)- (\omega+2k\alpha)\cdot\cos(2k\alpha\,t)+ e^{-\omega_0\delta t}\left[\omega_0\delta\sin\omega t + (\omega+2k\alpha)\cdot\cos\omega t\right]}{2\left[(\omega_0\delta)^2 + (\omega+2k\alpha)^2\right]} \left.\left.\left.\right]\right]\right\} \tag{B7}$$

$$I_3 = -\frac{4\,ab\,P_0}{mn\,\pi^2 M\omega}(\sin\frac{m\pi D}{a}) \cdot \int_{\sigma=0}^t \sum_{k=0}^\infty \left[\left[J_{2k+1}\left(\frac{m\pi H}{a}\right)\right]e^{\omega_0\delta(\sigma-t)}\sin\omega(\sigma-t) \sin((2k+1)\,\alpha\sigma)\,d\sigma\right]$$

$$I_3 = \frac{4\,ab\,P_0}{mn\pi^2 M\omega}(\sin\frac{m\pi D}{a})\left\{\sum_{k=0}^\infty\left[\left[J_{2k+1}\left(\frac{m\pi H}{a}\right)\right]\left[\right.\right.\right.$$

$$+\frac{(\omega - (2k+1)\alpha)\cdot\sin((2k+1)\alpha\,t)-\omega_0\delta\cos((2k+1)\cdot\alpha\,t)- e^{-\omega_0\delta t}\left[(\omega-(2k+1)\alpha)\sin\omega t - \omega_0\delta\cos\omega t\right]}{2\left[(\omega_0\delta)^2 + (\omega-(2k+1)\alpha)^2\right]} +$$

$$+\frac{(\omega + (2k+1)\alpha)\cdot\sin((2k+1)\alpha\,t)+\omega_0\delta\cos((2k+1)\cdot\alpha\,t)+ e^{-\omega_0\delta t}\left[(\omega+(2k+1)\alpha)\sin\omega t -\omega_0\delta\cos\omega t\right]}{2\left[(\omega_0\delta)^2 + (\omega+(2k+1)\alpha)^2\right]} \left.\left.\left.\right]\right]\right\} \tag{B8}$$

$$\xi_{osc_{mn}}(t) = \frac{2\,ab\,P_0}{mn\pi^2 M\omega^2}\left\{(\cos\frac{m\pi D}{a})\left[\left[1-J_0(\frac{m\pi H}{a})\right]\left[\left(\frac{\omega}{\omega_0}\right)^2 - e^{-\omega_0\delta t}\left[\frac{\omega\delta}{\omega_0}\sin\omega t +\left(\frac{\omega}{\omega_0}\right)^2\cdot\cos\omega t\right]\right]\right.\right.$$

$$-\,\omega\sum_{k=0}^{\infty}\left\{\left[J_{2k}(\frac{m\pi H}{a})\right]\left[\frac{\omega_0\delta\sin 2k\alpha t + (\omega-2k\alpha)\cos 2k\alpha t - e^{-\omega_0\delta t}\left[\omega_0\delta\sin\omega t + (\omega-2k\alpha)\cos\omega t\right]}{(\omega_0\delta)^2 + (\omega-2k\alpha)^2}\right.\right.$$

$$\left.\left.\left.-\frac{\omega_0\delta\sin 2k\alpha t - (\omega+2k\alpha)\cos 2k\alpha t + e^{-\omega_0\delta t}\left[\omega_0\delta\sin\omega t + (\omega-2k\alpha)\cos\omega t\right]}{(\omega_0\delta)^2 + (\omega+2k\alpha)^2}\right]\right\}\right]$$

$$+\,\omega(\sin\frac{m\pi D}{a})\cdot\sum_{k=0}^{\infty}\left\{\left[J_{2k+1}(\frac{m\pi H}{a})\right]\left[\right.\right.$$

$$+\frac{(\omega-(2k+1)\alpha)\sin(2k+1)\alpha t - \omega_0\delta\cos(2k+1)\alpha t - e^{-\omega_0\delta t}\left[(\omega-(2k+1)\alpha)\sin\omega t - \omega_0\delta\cos\omega t\right]}{(\omega_0\delta)^2 + (\omega-(2k+1)\alpha)^2}$$

$$\left.\left.+\frac{(\omega+(2k+1)\alpha)\sin(2k+1)\alpha t + \omega_0\delta\cos(2k+1)\alpha t + e^{-\omega_0\delta t}\left[(\omega+(2k+1)\alpha)\sin\omega t - \omega_0\delta\cos\omega t\right]}{(\omega_0\delta)^2 + (\omega+(2k+1)\alpha)^2}\right]\right\}\right. \tag{B9}$$

If damping is small, $\delta \rightarrow 0$ and Equation (B9) reduces to:

$$\xi_{osc_{mn}}(t) = \frac{2\,ab\,P_0}{mn\pi^2 M\omega^2}\left\{\cos\frac{m\pi D}{a}\left[1-J_0(\frac{m\pi H}{a})\right]\left[1-\cos\omega_0 t\right]-\right.$$

$$-\,2\omega_0^2\sum_{k=1}^{\infty}\left[(J_{2k}(\frac{m\pi H}{a}))\frac{\cos 2k\alpha t - \cos\omega_0 t}{\omega_0^2 - (2k\alpha)^2}\right]+$$

$$\left.+\,2\omega_0(\sin\frac{m\pi D}{a})\cdot\sum_{k=0}^{\infty}\left(J_{2k+1}(\frac{m\pi H}{a})\right)\left[\frac{\omega_0\sin(2k+1)\alpha t - (2k+1)\alpha\sin\omega_0 t}{\omega_0^2 - \alpha^2}\right]\right\} \tag{B10}$$

32

For large time, $t \rightarrow \infty$ and Equation (B9) reduces to:

$$\xi_{osc_{mn}}(t) = \frac{2 ab P_0}{mn \pi^2 M\omega^2} \left\{ (\cos \frac{m\pi D}{a}) \left[\left[1 - J_0 (\frac{m\pi H}{a}) \right] \left(\frac{\omega}{\omega_0} \right)^2 \right. \right.$$

$$- \omega \sum_{k=1}^{\infty} \left[J_{2k} (\frac{m\pi H}{a}) \right] \left[\frac{\omega_0 \delta \sin 2kat + (\omega - 2ka) \cos 2kat}{(\omega_0 \delta)^2 + (\omega - 2ka)^2} \right.$$

$$\left. \left. - \frac{\omega_0 \delta \sin 2kat - (\omega + 2ka) \cos 2kat}{(\omega_0 \delta)^2 + (\omega + 2ka)^2} \right] \right]$$

$$+ \omega (\sin \frac{m\pi D}{a}) \sum_{k=0}^{\infty} \left[J_{2k+1} (\frac{m\pi H}{a}) \right] \left[\frac{(\omega - (2k+1)a)\sin(2k+1)at - \omega_0 \delta \cos (2k+1)at}{(\omega_0 \delta)^2 + (\omega - 2k+1)a)^2} \right.$$

$$\left. \left. + \frac{(\omega + (2k+1)a)\sin(2k+1)at + \omega_0 \delta \cos (2k+1)at}{(\omega_0 \delta)^2 + (\omega + (2k+1)a)^2} \right] \right\}$$

$$\text{(B11)}$$

It is interesting to compare Equations (B9), (B10), and (B11) with (45), (46), and (47) respectively. It is observed that the first terms of the series in Equation (B11) (when k = 1 in the first sum, and k = 0 in the second sum) bare a strong resemblance to Equation (47). In fact, Equation (47) differs from the first terms of Equation (B11) in that (47) the factor $2(1-J_0 (\frac{m\pi H}{a}))$ is replaced by $(1 - \cos \frac{m\pi H}{a})$, the factor $2J_2 (\frac{m\pi H}{a})$ is

is replaced by $\frac{1}{2} \left[1 - \cos \frac{m\pi H}{a} \right]$ and the factor $2J_1 \left(\frac{m\pi H}{a} \right)$ is replaced by $\sin \frac{m\pi H}{a}$.

The agreement between equation (41) and the first terms of equation (B11) is very good provided $\frac{m\pi H}{a}$ is not too large, as the following example illustrates.

33

For $\frac{m\pi H}{a} = 0.5$: -

(i) $2\left[1 - J_0\left(\frac{m\pi H}{a}\right)\right] = 0.1231$; $\quad 1 - \cos\frac{m\pi H}{a} = 0.1224$

(ii) $2 J_2\left(\frac{m\pi H}{a}\right) = 0.0612$; $\quad \frac{1}{2}\left[1 - \cos\frac{m\pi H}{a}\right] = 0.0612$

(iii) $2 J_1\left(\frac{m\pi H}{a}\right) = 0.4845$; $\quad \sin\frac{m\pi H}{a} = 0.4794$

It may be observed that for $\frac{m\pi H}{a} = \pi/2$ the agreement is not nearly so good, and the agreement becomes progressively worse as the value of $\frac{m\pi H}{a}$ is increased.

It is also interesting to note that for small values of $\frac{m\pi H}{a}$ it is sufficiently accurate to consider only the first terms of the series in Equation (B11). This is obvious from an examination of the figure below:

Values of x
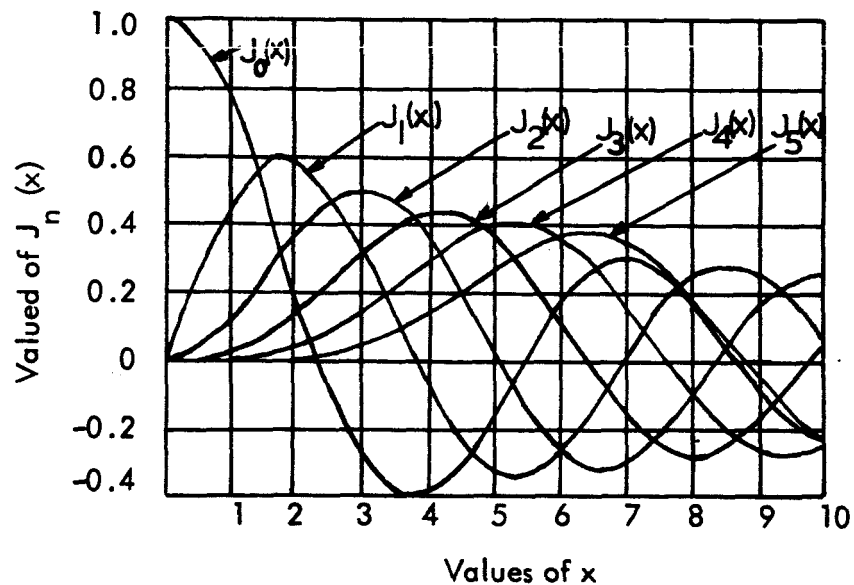
This figure shows that the second terms of the series in Equation (B11) start to become significant as $\frac{m\pi H}{a} \longrightarrow \pi/2$. When $\frac{m\pi H}{a} = \pi$, the largest value which needs to be considered for the first mode (m = 1), the second terms are appreciable and in fact $J_1(\pi) \approx J_3(\pi)$. For higher modes (m > 1) the higher order Bessel functions become appreciable rapidly for smaller values of $\frac{m\pi H}{a}$ and can no longer be neglected.

One other interesting observation, which can be made by examining Equation (B11), is that not only do first mode resonances occur for excitation by a shock wave oscillating at the resonant angular frequency ω and the "sub-harmonic" frequency $\omega/2$

34

as is shown by Equation (47) , but that they also occur for excitation by an infinite number of "sub-harmonic" frequencies $\omega/3$, $\omega/4$, $\omega/5$ ....etc.   However, the response in the first mode due to these higher "sub-harmonic" forcing frequencies is only appreciable for large amplitude shock oscillations; the response in the higher modes to the higher "sub-harmonic" frequencies becomes appreciable for much smaller amplitude shock oscillations.

APPENDIX C

FORMULATION OF PANEL RESPONSE THEORY FOR PANELS WITH CLAMPED-CLAMPED EDGES

It is not possible in the case of a panel with clamped-clamped edges to write down a mathematical expression for the mode shape which exactly satisfies all the boundary conditions. However, a good engineering approximation is given by:

$$f_r(x,y) = f_{mn}(x,y) = \frac{X_m X_n}{|X_m||X_n|}$$

$$f_r(x,y) = \frac{1}{|X_m||X_n|}\left[A_m \cosh\frac{\alpha_m x}{a} + B_m \sinh\frac{\alpha_m x}{a} + C_m \cos\frac{\alpha_m x}{a} + D_m \sin\frac{\alpha_m x}{a}\right] \cdot$$

$$\cdot \left[A_n \cosh\frac{\alpha_n y}{b} + B_n \sinh\frac{\alpha_n y}{b} + C_n \cos\frac{\alpha_n y}{b} + D_n \sin\frac{\alpha_n y}{b}\right]$$

(C.1)

where X_m, X_n are the mode shapes in the x- and y-directions and $|X_m|$, $|X_n|$ are their maximum values respectively; and A_m, B_m, C_m, D_m, A_n, B_n, C_n, and D_n are modal coefficients which are determined by the boundary conditions of the panel. Applying the boundary conditions for a clamped-clamped panel, that is that for X_m and

X_n, $X_m = \dfrac{\partial X_m}{\partial x} = X_n = \dfrac{\partial X_n}{\partial y} = 0$, for $x = a$ and $y = b$ and for $x = y = 0$,

respectively.

$$\left.\begin{aligned}
A &= -C \\
B &= -D \\
0 &= A \cosh\alpha + B \sinh\alpha + C \cos\alpha + D \sin\alpha \\
0 &= A \sinh\alpha + B \cosh\alpha - C \sin\alpha + D \cos\alpha
\end{aligned}\right\} \quad (C.2)$$

Equations (C.2) may be solved in order to obtain the frequency equation for a clamped-clamped panel:

$$\cosh \alpha_n \cos \alpha_m = 1$$

$$\cosh \alpha_n \cos \alpha_n = 1$$

$$\left.\begin{array}{c}\\\\\\\\\end{array}\right\} \qquad \text{(C.3)}$$

The mode shape $f_r(x,y)$ defined in equation (C.1) above is used in equation (4) and wherever else required instead of $\sin\dfrac{m\pi y}{a} \sin\dfrac{n\pi y}{b}$, if analysis is required for a clamped-clamped panel instead of a simply supported panel. The other parameters required are discussed below and the necessary parameters which were calculated in Reference 15 are given in Table 1.

The natural resonant angular frequencies, which for a simply-supported panel are given by equation (28), are given for a clamped-clamped panel by:

$$\omega_{mn} = \frac{h}{b^2} \sqrt{R_{mn}} \sqrt{\frac{E}{12\rho(1 - \nu^2)}} \qquad \text{(C.4)}$$

where

$$R_{mn} = \left(\frac{b}{a}\right)^4 \cdot \alpha_m{}^4 + \alpha_n{}^4 + 2\left(\frac{b}{a}\right)^2 \cdot \psi_m \psi_n \qquad \text{(C.5)}$$

where ψ_m, ψ_n are resonant frequency parameters which are defined and evaluated in Reference 15 and given in Table 1 below.

The generalized mass, which for a simply-supported panel is given by equation (29), is given for a clamped-clamped panel by:

$$M_{mn} = M_m M_n (\rho h a b) \qquad \text{(C.6)}$$

where

$$M_m = \int_0^a \left[\frac{X_m}{|X_m|}\right]^2 dx \; ; \qquad M_n = \int_0^b \left[\frac{X_n}{|X_n|}\right]^2 dy \qquad \text{(C.7)}$$

Although the modal constants, frequency parameters and generalized mass have been calculated for a clamped-clamped beam for the first few modes and are presented in several references (for example the first five modes are given in Reference 19), these parameters are required for at least the first nine or ten modes for the analysis of panel response. Thus, these parameters were calculated in Reference 15, and are presented here in Table 1.

m or n	Generalized Mass M_m or M_n	Frequency Parameter a_m or a_n	Resonant Frequency Parameter ψ_m or ψ_n	Maximum Displacement X_m or X_n	Modal Coefficient A_m or A_n
1	0.396	4.73004	12.302	1.61628	1.017804
2	0.439	7.85320	46.050	1.50805	0.999224
3	0.436	10.99560	98.905	1.51259	1.000034
4	0.420	14.13720	171.590	1.51228	0.999998552
5	0.437	17.27880	264.1376	1.5125	1.0000000627
6	0.437	20.420352	376.1092	1.5125	0.9999999729
7	0.437	23.561945	506.8632	1.5125	1.000000001175
8	0.437	26.703537	659.4048	1.5125	0.999999999491
9	0.437	29.845130	830.7431	1.5125	1.0000000000000220
10	0.437	32.986722		1.5125	0.9999999999999066

Table 1.   Parameters for a Clamped – Clamped Mode Shape

It should be noted that the modal coefficients: $C_m = -A_m$, $C_n = -A_n$ and $B_m = -D_n = -1$. More significant figures are given in Table 1 above where they are required for accurate calculations.

APPENDIX D

LOGIC FOR THE DIGITAL COMPUTER PROGRAM

Equation (47) may be written as amplification factor A for the first mode (by dividing by the first term of Equation (31) and putting m = 1):

$$A = \frac{1}{4(1-\delta^2)}\left\{ (\cos \pi \bar{D})(1 - \cos \pi \bar{H}) \left[1-\delta^2 - \frac{\frac{\delta}{\sqrt{(1-\delta^2)}}\sin 2\bar{\sigma} + (1-\frac{2\alpha}{\omega})\cos 2\bar{\sigma}}{2\left[\frac{\delta 2}{1-\delta^2} + (1 - \frac{2\alpha}{\omega})^2\right]} - \right.\right.$$

$$\left. - \frac{\frac{\delta}{\sqrt{(1-\delta^2)}}\sin 2\bar{\sigma} + (1+\frac{2\alpha}{\omega})\cos 2\bar{\sigma}}{2\left[\frac{\delta^2}{1-\delta^2} + (1+\frac{2\alpha}{\omega})^2\right]}\right] + 2(\sin \pi \bar{D})(\sin \pi \bar{H})\left[\frac{(1-\frac{\alpha}{\omega})\sin\bar{\sigma} - \frac{\delta}{\sqrt{(1-\delta^2)}}\cos\bar{\sigma}}{2\left[\frac{\delta^2}{1-\delta^2} + (1-\frac{\alpha}{\omega})^2\right]} + \right.$$

$$\left.\left. + \frac{(1+\frac{\alpha}{\omega})\sin\bar{\sigma} + \frac{\delta}{\sqrt{(1-\delta^2)}}\cos\bar{\sigma}}{2\left[\frac{\delta^2}{1-\delta^2} + (1+\frac{\alpha}{\omega})^2\right]}\right]\right\} \tag{D1}$$

where $\bar{D} = D/a$, $\bar{H} = H/a$, and $\bar{\sigma} = \alpha t$

Putting $\alpha/\omega = \beta$ and neglecting second order terms in δ, since δ is small gives:

$$A = \frac{1}{8}\left\{ (\cos \pi \bar{D})(1-\cos \pi \bar{H}) \left[1 - \frac{\delta \sin 2\bar{\sigma} + (1-2\beta)\cos 2\bar{\sigma}}{\delta^2 + (1-2\beta)^2} - \frac{\delta \sin 2\bar{\sigma} - (1+2\beta)\cos 2\bar{\sigma}}{\delta^2 + (1+2\beta)^2}\right] + \right.$$

$$\left. + 2(\sin \pi \bar{D})(\sin \pi \bar{H})\left[\frac{(1-\beta)\sin\bar{\sigma} - \delta\cos\bar{\sigma}}{\delta^2 + (1-\beta)^2} + \frac{(1+\beta)\sin\bar{\sigma} + \delta\cos\bar{\sigma}}{\delta^2 + (1+\beta)^2}\right]\right\} \tag{D2}$$

The computer program was written to compute Equation (D2) as time $\bar{\sigma}$ varied between 0 and 2π. The maximum and minimum values of A where chosen for each case under consideration. The parameters which were varied and the values assigned are given below:

40

δ = 0.005, 0.010 and 0.020 ;

$\bar{D}$ = 0.0 , 0.1 , 0.2 , 0.3 , 0.4 , and 0.5 ;

$\bar{H}$ = 0.0 , 0.1 , 0.2 , 0.3 , 0.4 , and 0.5 ;

β = 1.050, 1.020, 1.010, 1.005, 1.002, 1.001, 1.000, 0.999, 0.998, 0.995, 0.990, 0.980, 0.950, 0.525, 0.510, 0.505, 0.5025, 0.5010, 0.5005, 0.5000, 0.4995, 0.4990, 0.4975, 0.4950, 0.4900, 0.4750.

The flow chart which was used to calculate the values of maximum A for these cases is given in Figure D1 following. Figure D2 gives the listing of the computer program which was written.
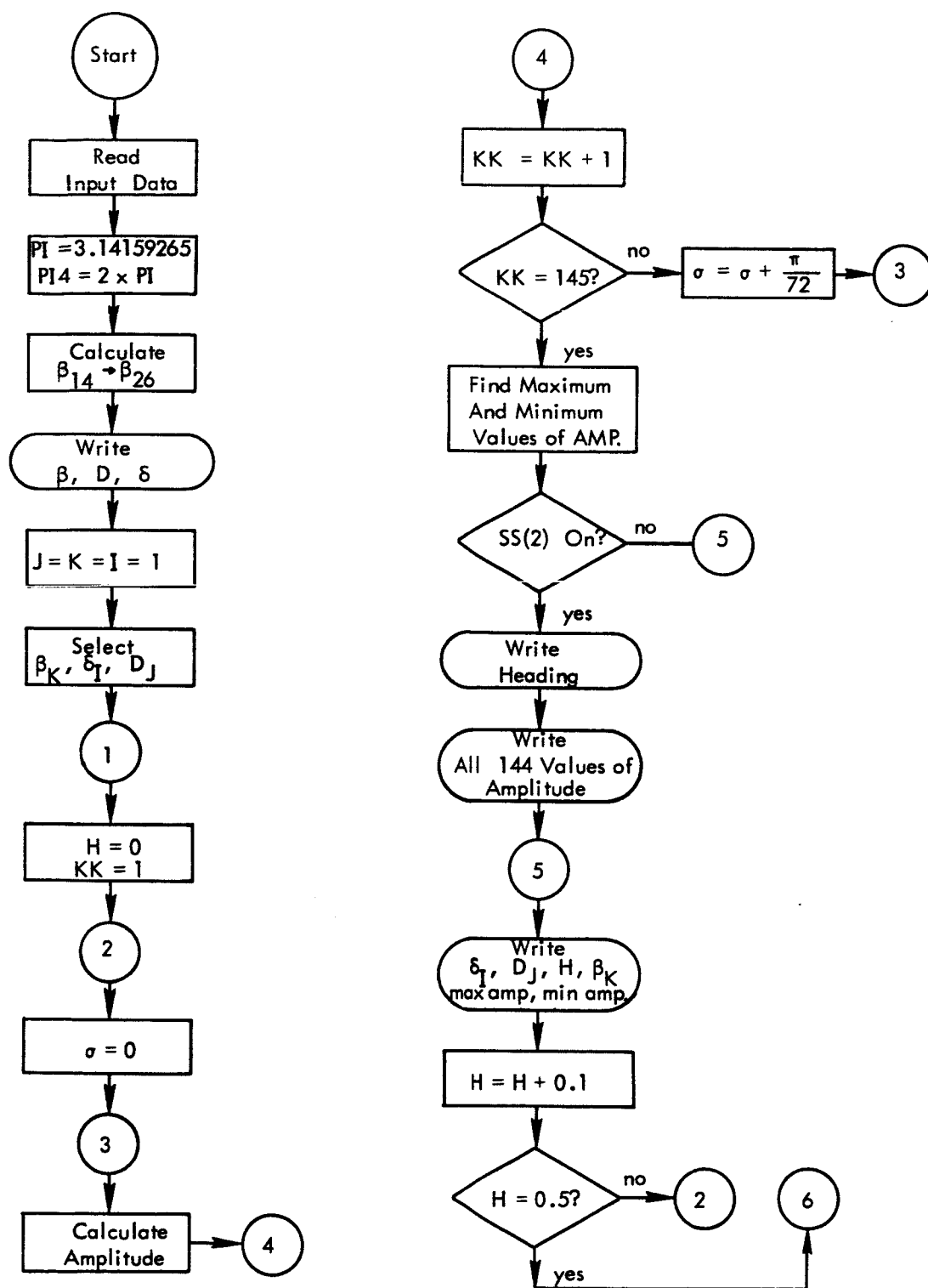
Figure D1. Flow Chart to Solve Computer Program
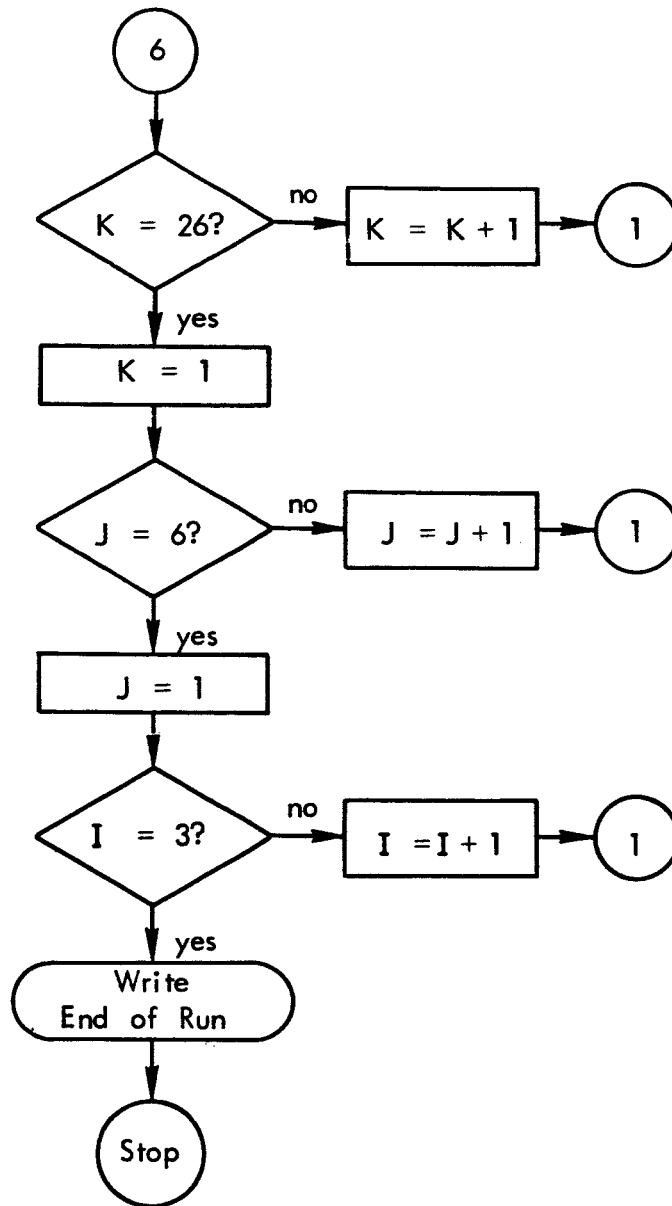
Figure D1. (Continued)

```
      PROGRAM MALCOLM
      COMMON A(144),BETA(26),DEE(6),DELTA(3),SIGMA
      PI=3.14159265
C     CALCULATION OF PANEL DYNAMIC AMPLIFICATION FACTORS DUE TO
C     SINUSOIDALLY OSCILLATING SHOCK
C     DATA SHOULD BE PREPARED AS FOLLOWS
C     13 VALUES OF BETA,SIX PER CARD,FORMAT (6F12.6)
C     6 VALUES OF D   ,SIX PER CARD,FORMAT(6F12.6)
C     3 VALUES OF DELTA, 3 PER CARD,FORMAT(6F12.6)
      PI4=4.*PI
      READ(60,100)(BETA(I),I=1,6)
      READ(60,100)(BETA(I),I=7,12)
      READ(60,100) BETA(13)
      DO 33 JKK=14,26
   33 BETA(JKK)=BETA(JKK-13)/2.
      READ(60,100)(DEE(I),I=1,6)
      READ(60,100)(DELTA(I),I=1,3)
      WRITE (61,699)
      WRITE (61,700) (BETA(IX),IX=1,26),(DEE(IXX),IXX=1,6),(DELTA(IIX),
     1IIX=1,3)
      DO 190 I=1,3
      DO 190 II=1,6
      DO 190 III=1,26
      HH=0.
      DO 81 KK=1,6
      K=1
      SIGMA=0.
    5 XX1=COSF(PI*DEE(II))*(1.-COSF(PI*HH))
      DELT2=DELTA(I)*DELTA(I)
      XX2=1.-(DELTA(I)*SINF(2.*SIGMA)+(1.-2.*BETA(III))*COSF(2.*SIGMA))/
     1(DELT2+(1.-2.*BETA(III))**2)-(DELTA(I)*SINF(2.*SIGMA)-(1.+2.*BETA(
     2III))*COSF(2.*SIGMA))/(DELT2+(1.+2.*BETA(III))**2)
      XX3=2.*SINF(PI*DEE(II))*SINF(PI*HH)*(((1.-BETA(III))*SINF(SIGMA)-
     1DELTA(I)*COSF(SIGMA))/(DELT2+(1.-BETA(III))**2)+((1.+BETA(III))*
     2SINF(SIGMA)+DELTA(I)*COSF(SIGMA))/(DELT2+(1.+BETA(III))**2))
      A(K)=(.125)*(XX1*XX2+XX3)
      K=K+1
      IF(K.EQ.145)82,83
   83 SIGMA=SIGMA+PI/72.
      GO TO 5
   82 VALMAX=VALMIN=A(1)
      DO 85 KKK=1,144
      IF(A(KKK).GT.VALMAX)1,2
    1 VALMAX=A(KKK)
      GO TO 85
    2 IF(A(KKK).LT.VALMIN)3,85
    3 VALMIN=A(KKK)
   85 CONTINUE
      GO TO (877,88),SSWTCHF(2)
  877 IF (HH.EQ..5) 87,88
   87 IF (II.EQ.1.AND.HH.EQ..5.AND.III.EQ.1.OR.III.EQ.13.OR.III.EQ.14.OR
     1.III.EQ.20.OR.III.EQ.26) 870,88
  870 WRITE (61,200) DELTA(I),DEE(II),HH,BETA(III)
      WRITE(61,300)(A(IK),IK=1,144)
   88 WRITE (61,800) DELTA(I),DEE(II),HH,BETA(III),VALMAX,VALMIN
   81 HH=HH+.1
  190 CONTINUE
      WRITE(59,400)
  100 FORMAT(6F12.3)
  200 FORMAT(2X,30HVALUES OF AMPLITUDE FOR DELTA=,E12.3,2X,2HD=,E12.3,
     12X,2HH=,E12.3,2X,9HAND BETA=,E12.3)
  300 FORMAT(12X,7E16.8)
  400 FORMAT(2X,10HEND OF RUN)
  800 FORMAT (5X,6HDELTA=,E12.6,3X,2HD=,E12.6,3X,2HH=,E12.6,3X,5HBETA=,
     1E12.6,3X,8HMAX AMP=,E16.8,3X,8HMIN AMP=,E16.8)
  699 FORMAT (20X,10HINPUT DATA)
  700 FORMAT (2X,6F12.6)
      END
```

Figure D2. Computer Program

REFERENCES

1. Young, G. and Shiokari, T., "Buffeting Data Obtained on Mercury/Atlas MA-2 and MA-3", Report No. TDR 594 (1101) TN-1, August 1961.

2. Krause, F.R., "Preliminary Results of SA-4 Acoustic Flight Tests", MSFC, Huntsville, Alabama, Memo M-Aero-A-48-63, May 1963.

3. Ellingwood, J.W. et al, "Shock-Wave Oscillations in Supersonic Flow", WADC Technical Note 57-409, December 1957.

4. Kistler, A.L., "Fluctuating Wall Pressure Under a Separated Supersonic Flow", Journ. Acous. Soc. America Vol. 36, No. 3, March 1964, pp. 543-550.

5. Wilson, J., "Unpublished Data from Sled Tests Conducted at Holloman AFB, New Mexico", Wyle Laboratories, private communication, February 1966.

6. Lowson, M.V., "Prediction of Inflight Fluctuating Pressures on Space Vehicles", Wyle Laboratories - Research Staff Report WR 65-26, December 1965.

7. Lowson, M.V., "The Acoustic Environment Due to Separated Flow and Oscillating Shocks", Wyle Laboratories Quarterly Progress Report for April, May, and June 1965 on Contract NAS8-11308.

8. Timoshenko, S. and Wionowsky-Krieger, S., "Theory of Plates and Shells", McGraw-Hill Book Company, Inc., 1959, Chapters 1 and 2.

9. Timoshenko, S. and Young, D.H., "Advanced Dynamics", McGraw-Hill Book Company, Inc., 1948.

10. Measuring and Evaluation Section MSFC, "Vibration and Acoustic Analysis of Saturn SA-4 Flight", IN - P and VE-S-63-52, November 1963.

11. Jones, G.W. and Foughner, J.T., "Investigation of Buffet Pressures on Models of Large Manned Launch Vehicle Configurations", NASA TN D-1633, May 1963.

12. Burrington, R.S., "Handbook of Mathematical Tables and Formulas", McGraw-Hill Book Company, Inc., 1962.

13. Crocker, M.R. and White, R.W., "Some Integration Formulae which Simplify the Evaluation of Certain Integrals in Common Use by Engineers", Wyle Laboratories - Research Staff Technical Memorandum, March 1966, (in publication).

14. Ungar, E.E., "Response of Plates to Moving Shocks", WADD Technical Report 60-445, August 1960.

15. Crocker, M.J., "Theoretical and Experimental Response of Panels to Traveling Sonic Boom and Blast Waves", Wyle Laboratories – Research Staff Report WR 66-2, March 1966.

16. Crocker, M.J., "Multimode Response of Panels to Sonic Boom", Paper (Q6) given before the Seventeenth Meeting of the Acoustical Society of America, St. Louis, November 1965.

17. Crocker, M.J., "Multimode Response of Panels to Sonic Boom", Wyle Laboratories – Research Staff Report WR 66-1, January 1966.

18. Abramowitz, M. and Stegun, 1. A. (Editors), "Handbook of Mathematical Functions", National Bureau of Standards, June 1964.

19. Bishop, R.E.D. and Johnson D.C., "The Mechanics of Vibration", Chapter 7, Cambridge University Press, 1960.
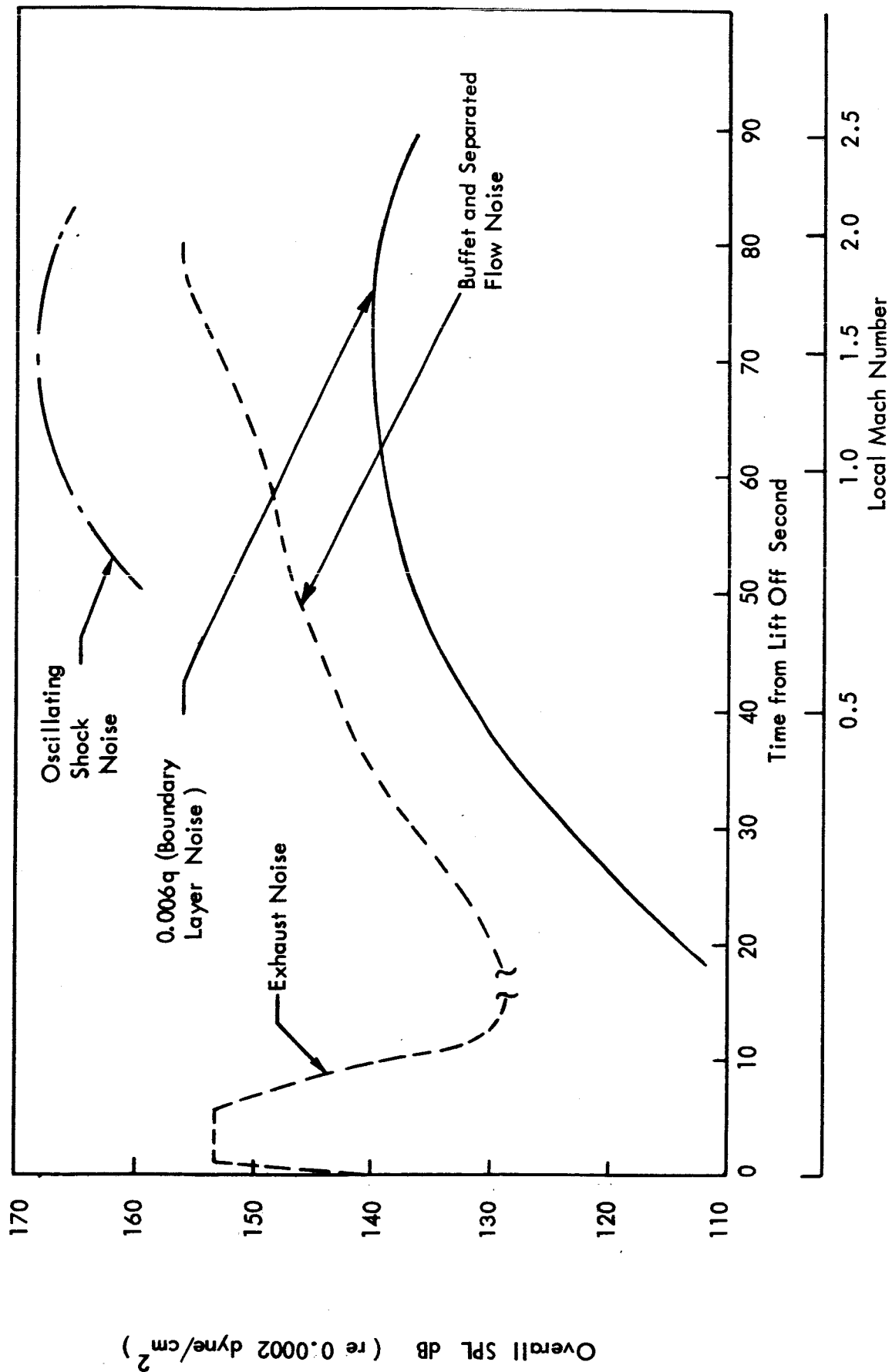
Figure 1. Relative Importance of Noise Sources Measured on the Structure of a Typical Large Space Vehicle (Extracted from Reference 2)

47
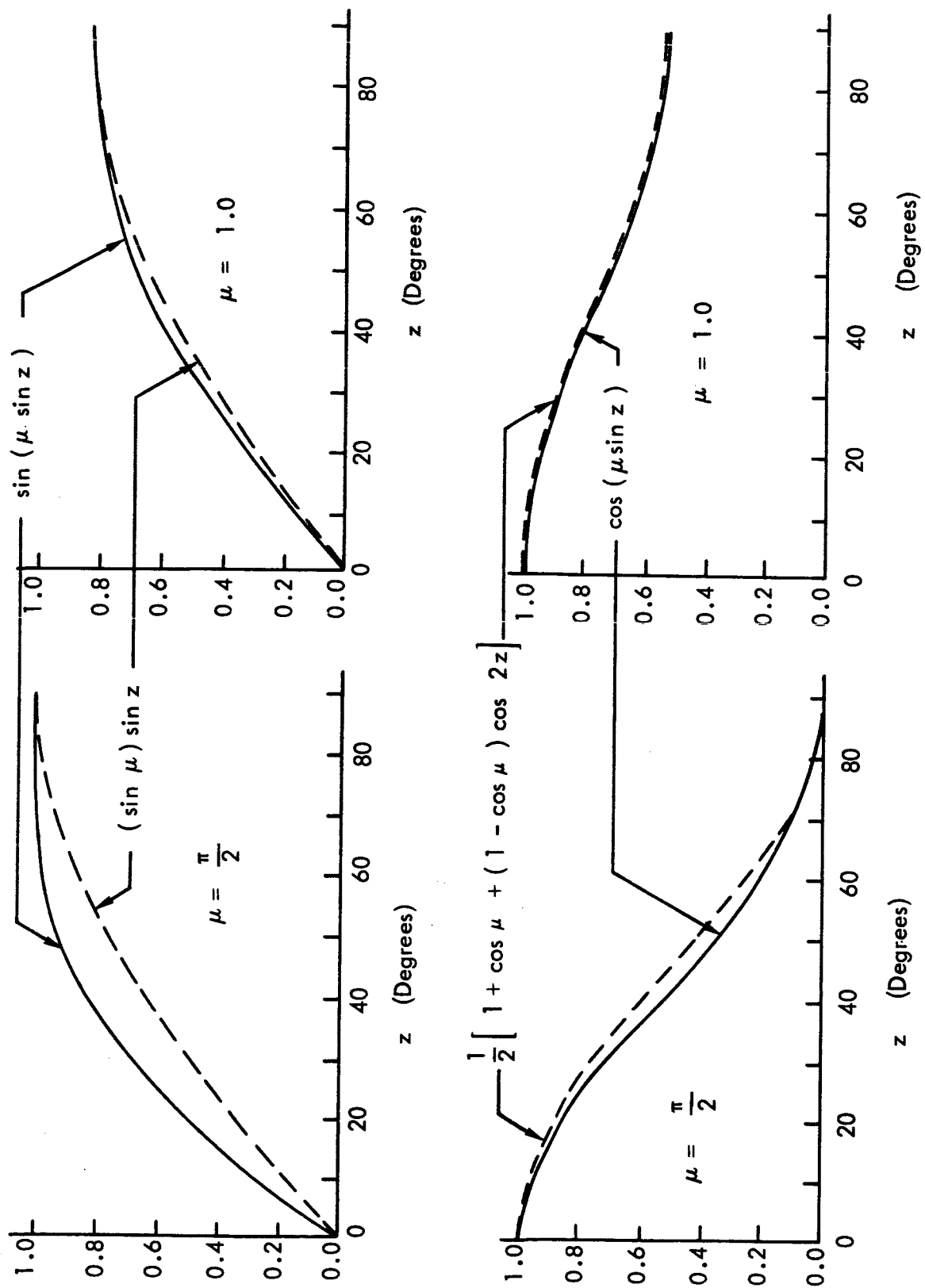
Figure 2.   Comparison of   sin (μ sin z) and   cos (μ sin z) to Approximating Functions

48
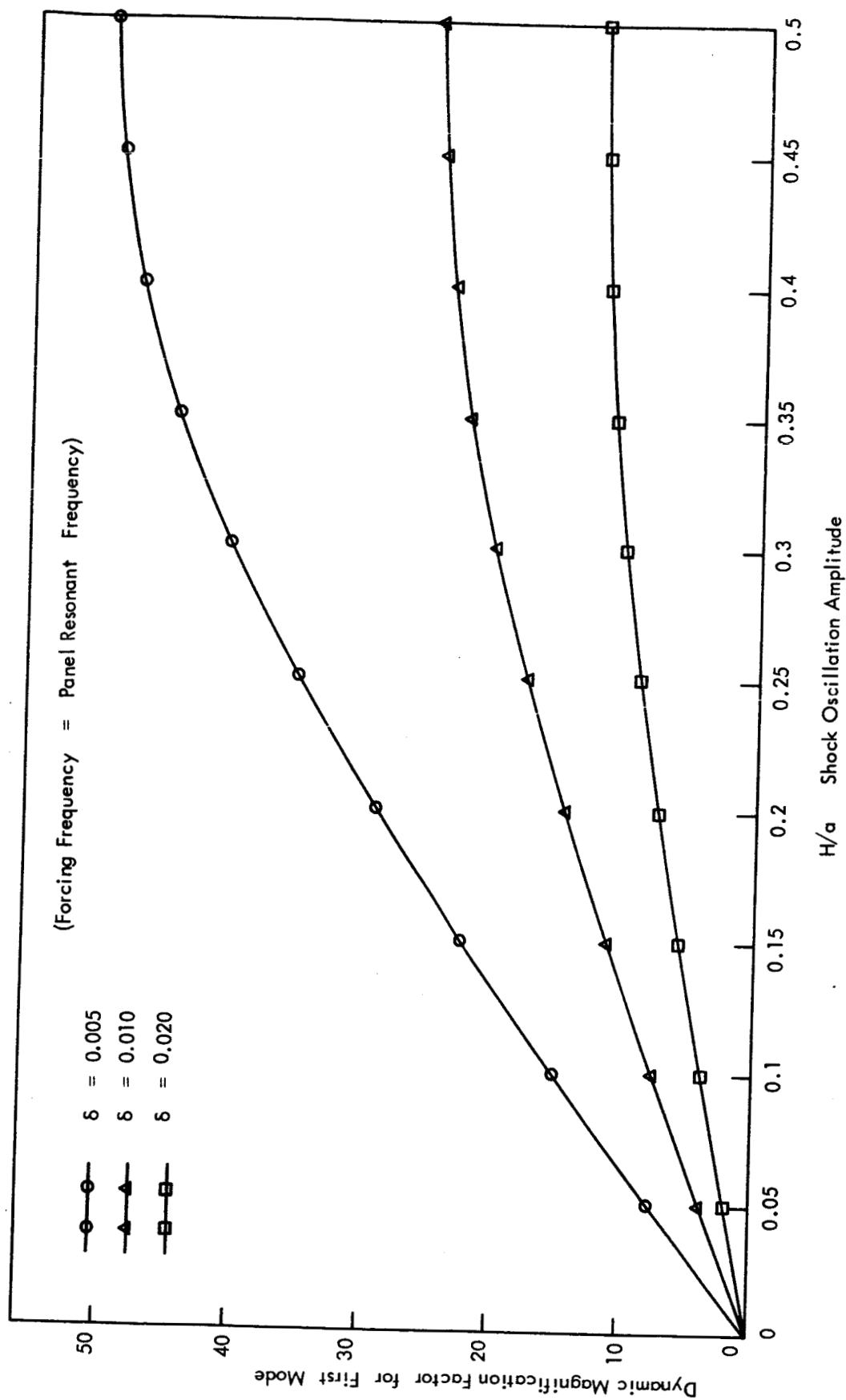
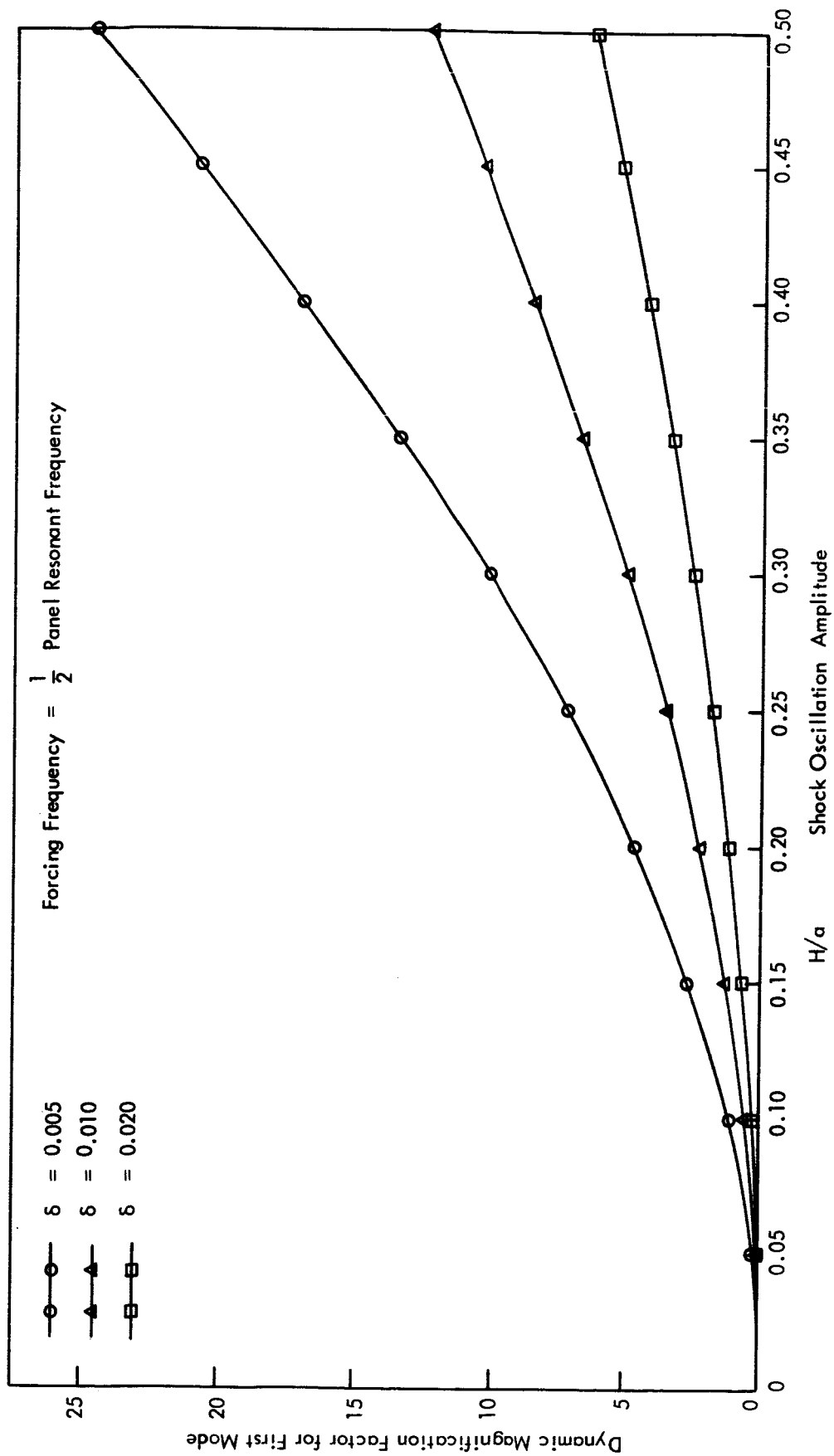Figure 3. Dynamic Magnification Factor for First Mode ~ Shock Oscillations About Panel Center

49

Figure 4. Dynamic Magnification Factor for First Mode ~ Shock Oscillations About Panel Edge
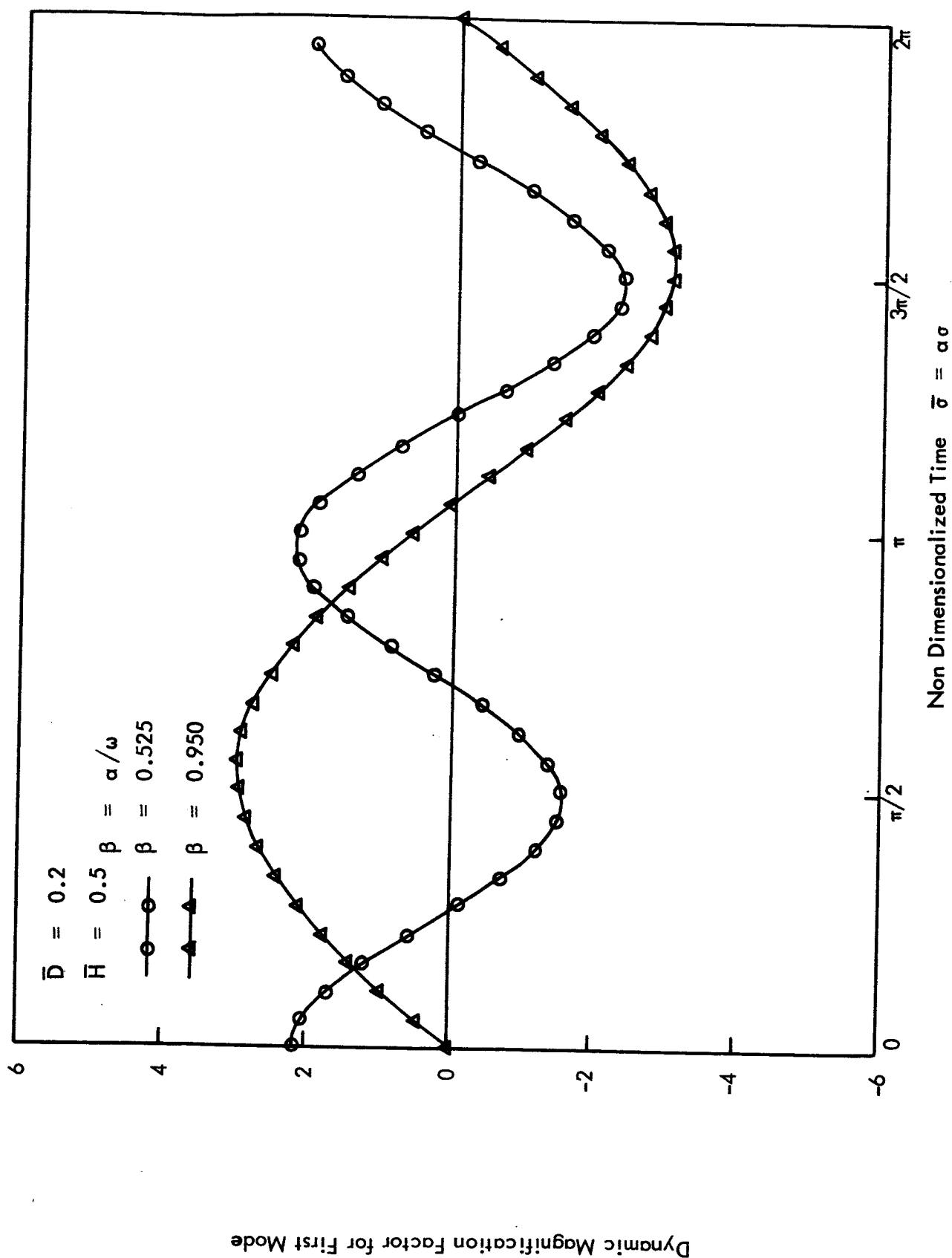
Figure 5.   Typical Amplitude Time History Curves for Panel Displacement

(δ = 0.005)

51
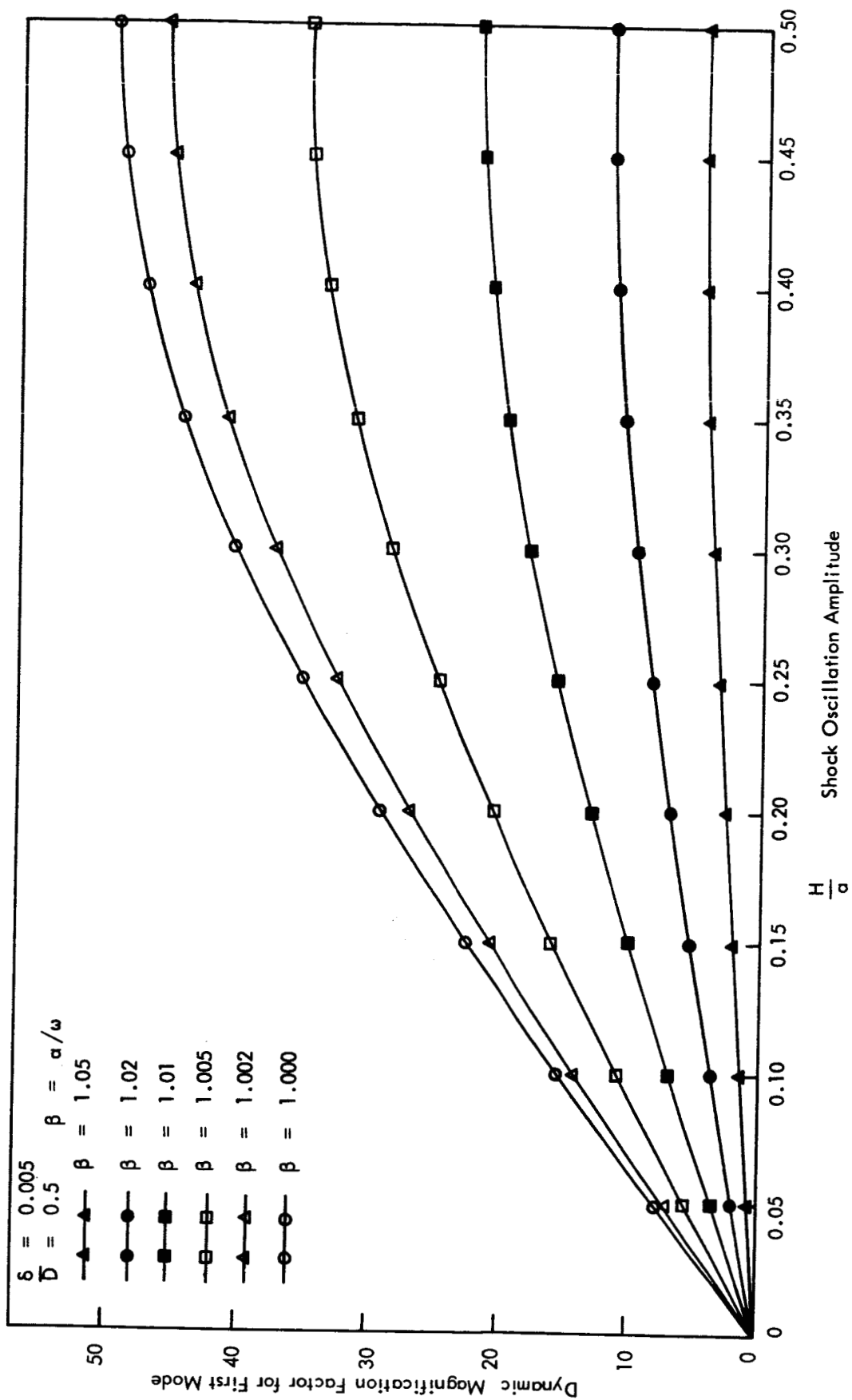
Figure 6. Dynamic Magnification Factor as a Function of Shock Oscillation Amplitude for Different Forcing Frequencies ~ Shock Oscillations About Panel Center ($\delta = 0.005$)

52
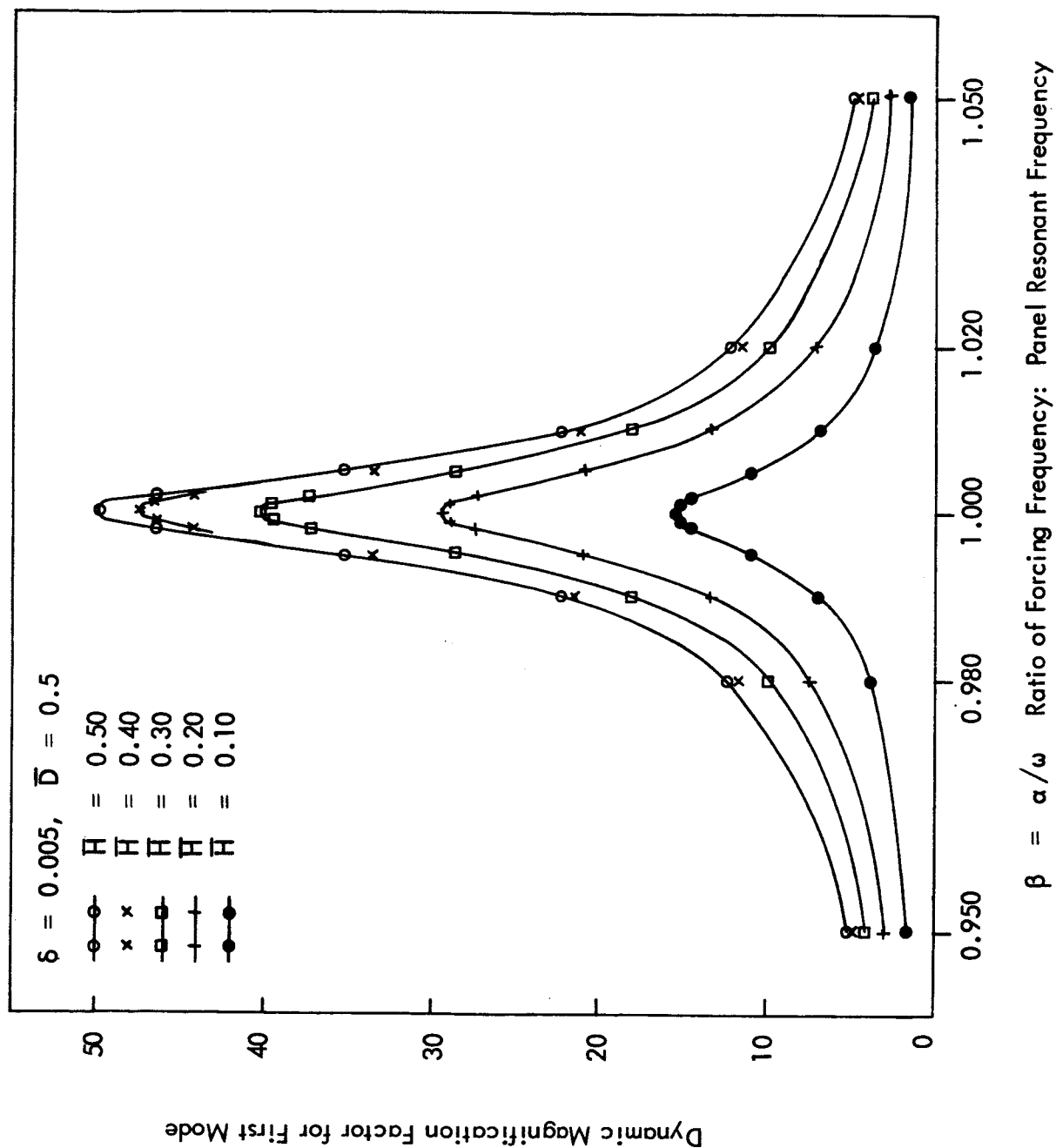
Figure 7. Dynamic Magnification Factor as a Function of Forcing Frequency for Different Shock Oscillation Amplitudes ~ Shock Oscillations About Panel Center (δ = 0.005)
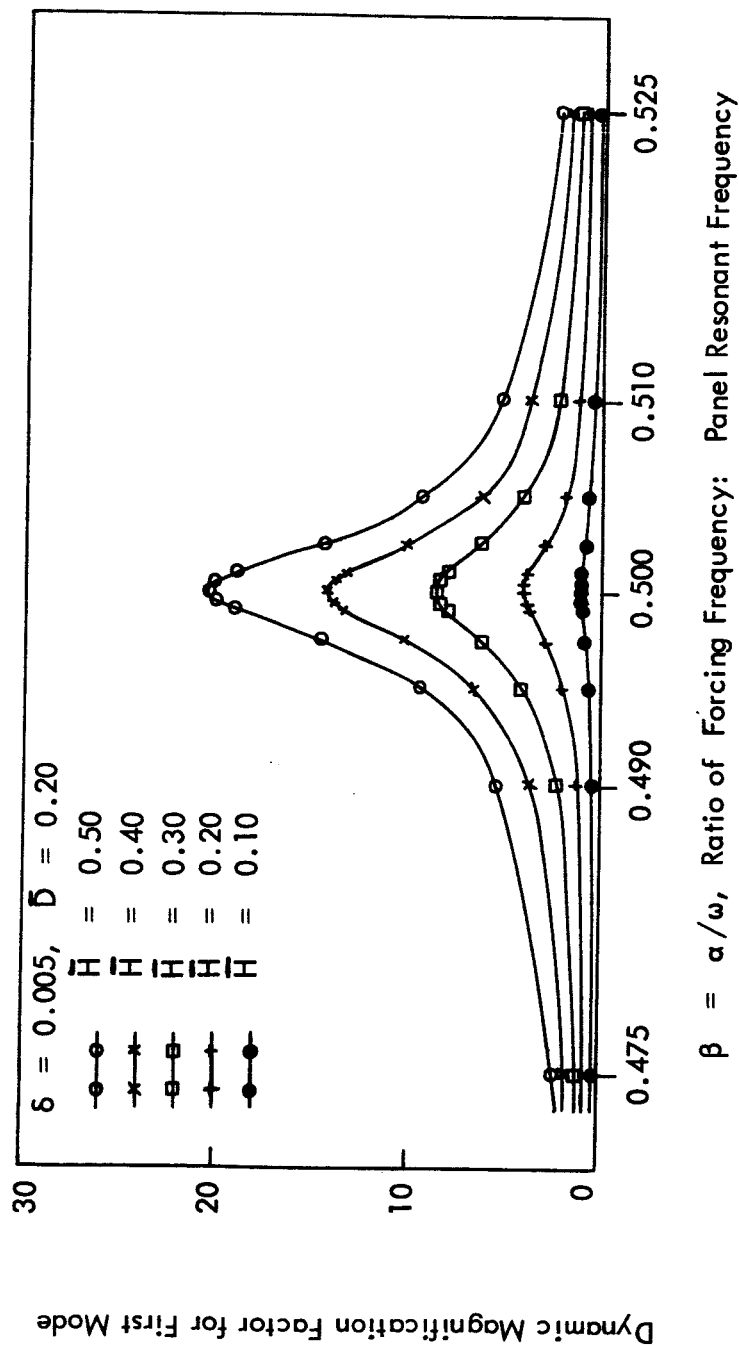
53

Figure 8. Dynamic Magnification Factor as a Function of Forcing Frequency for Different Shock Oscillation Amplitudes ~ Shock Oscillations About $\bar{D} = 0.20$ First Resonance ($\delta = 0.005$)
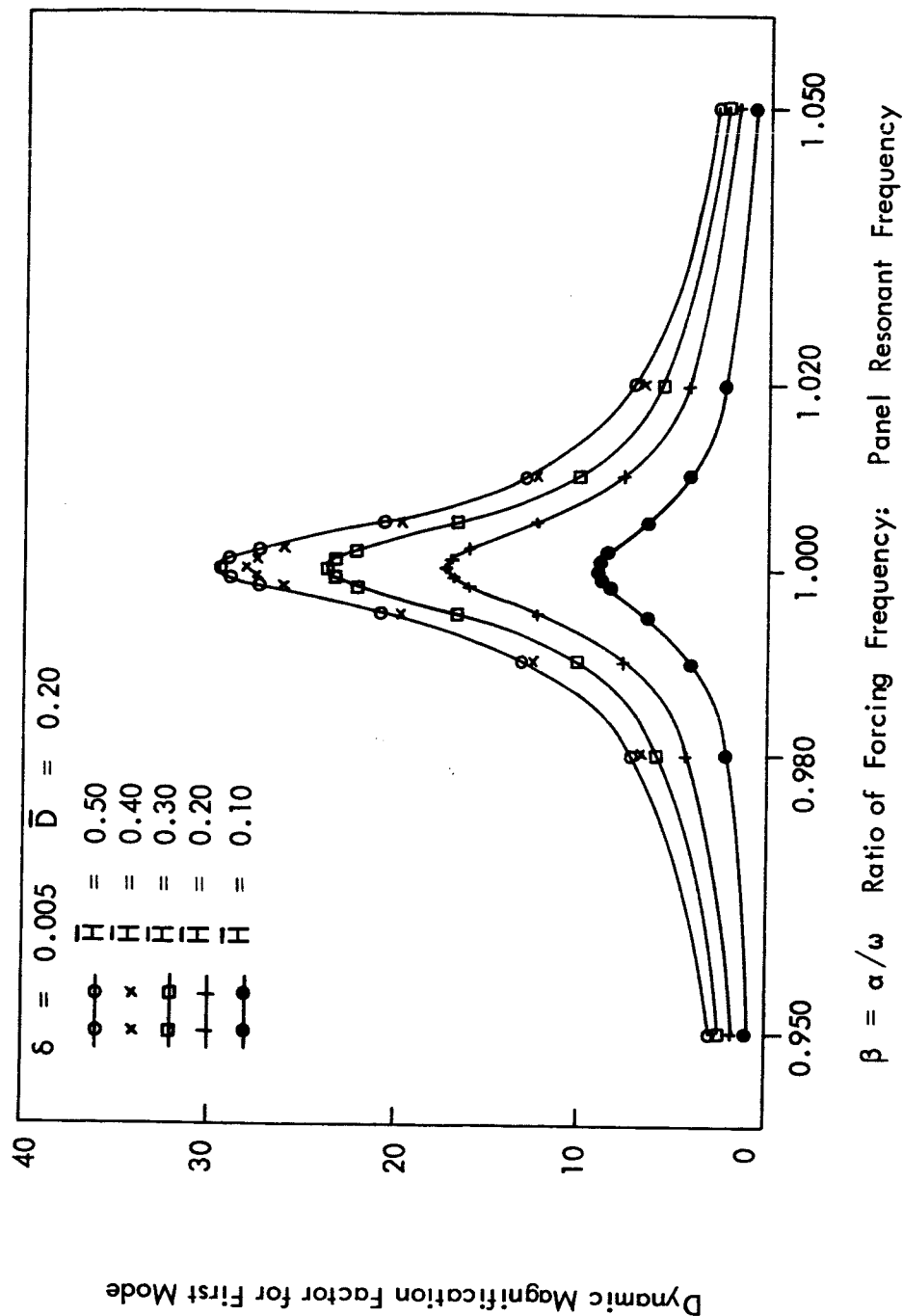
54

Figure 9. Dynamic Magnification Factor as a Function of Forcing Frequency for Different Shock Oscillation Amplitudes ~ Shock Oscillations About $\bar{D} = 0.20$. Second Resonance ($\delta = 0.005$)

55
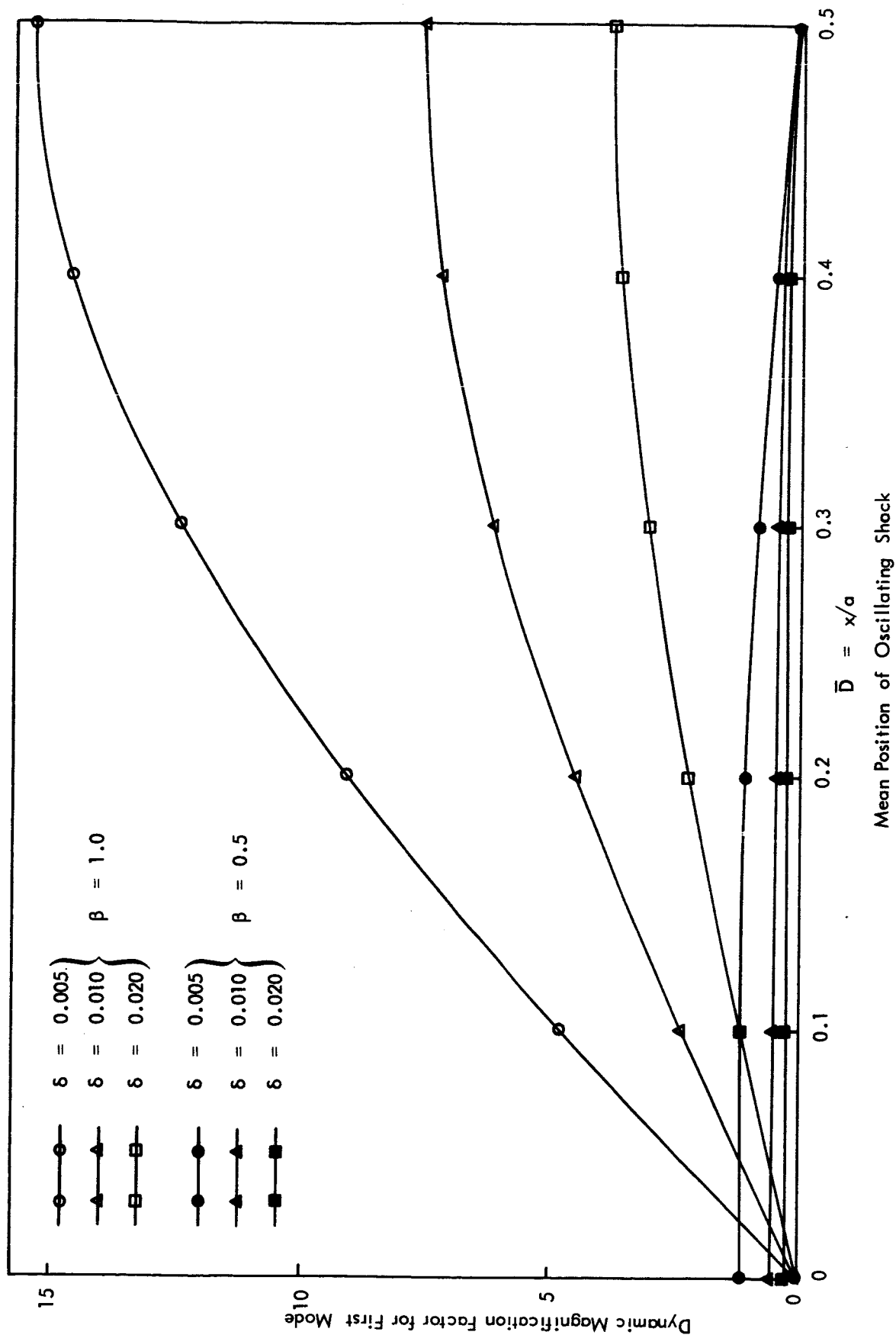
Figure 10. Dynamic Magnification Factor Against Mean Position of Oscillating Shock for Constant Shock Amplitude H/a = 0.1
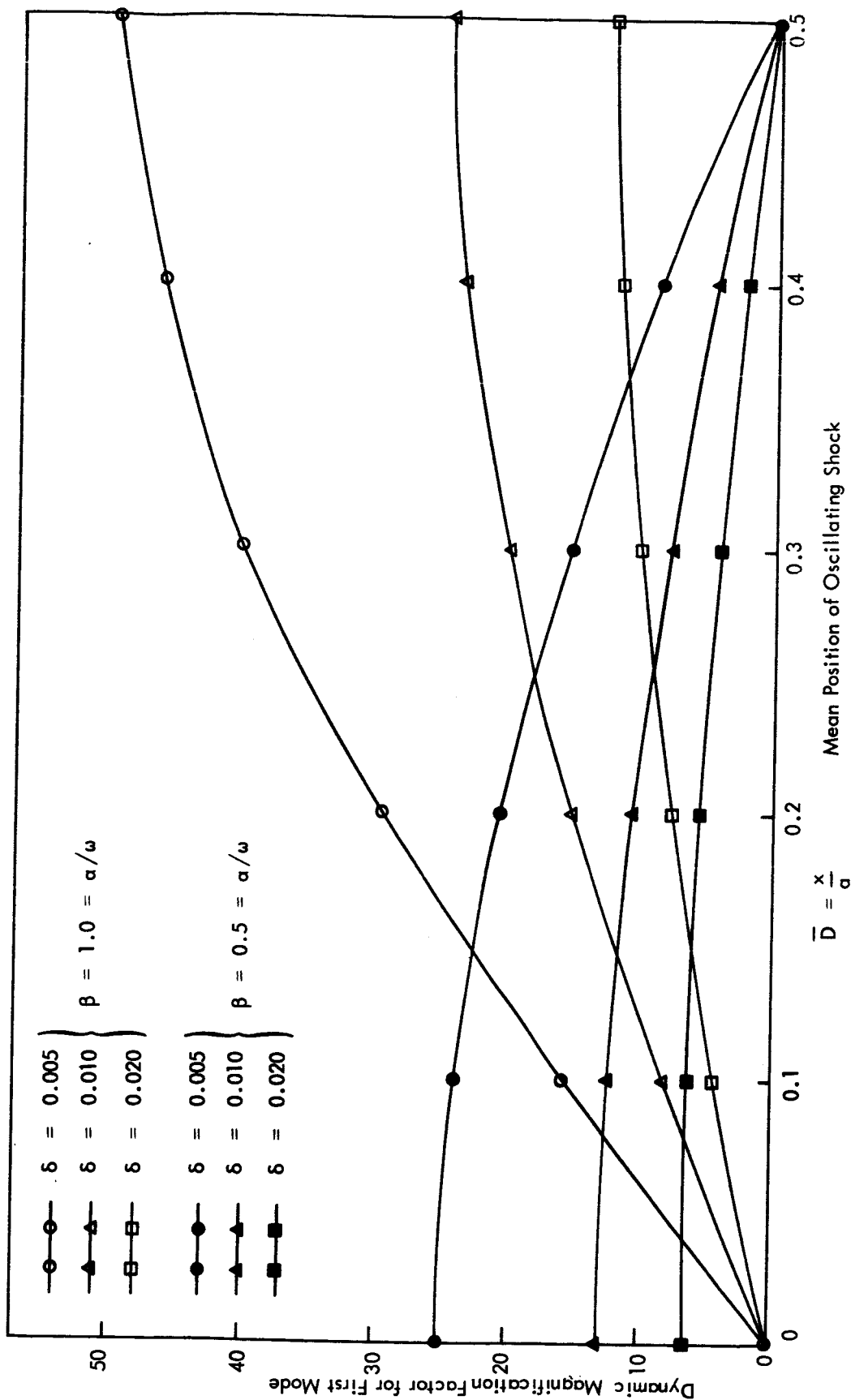
Figure 11. Dynamic Magnification Factor Against Mean Position of Oscillating Shock for Constant Shock Amplitude $\frac{H}{a} = 0.5$

57